2-1-2016

Fission Multiplicity Distribution Sampling in MCNP6 Criticality Calculations

Mario Ivan Ortega

Mario I. Ortega

Candidate

Nuclear Engineering

Department

This thesis is approved, and it is acceptable in quality and form for publication:

Approved by the Thesis Committee:

Dr. Anil K. Prinja, Chair

Dr. Robert D. Busch, Member

Dr. Forrest B. Brown, Member

Fission Multiplicity Distribution Sampling in MCNP6 Criticality Calculations

by

Mario I. Ortega

B.S., Nuclear Engineering, University of New Mexico, 2013

THESIS

Submitted in Partial Fulfillment of the
Requirements for the Degree of

Master of Science
Nuclear Engineering

The University of New Mexico

Albuquerque, New Mexico

December, 2015

Dedication

To my parents and brothers, for their support, encouragement, and patience.

Acknowledgments

I would like to thank my advisor, Dr. Anil Prinja for his patience, flexibility, and insightful conversations and observations. I would also like to thank Dr. Michael E. Rising and Dr. Forrest B. Brown for their support, willingness to answer questions, and generally tolerating my incessant emails.

Fission Multiplicity Distribution Sampling in MCNP6 Criticality Calculations

by

Mario I. Ortega

B.S., Nuclear Engineering, University of New Mexico, 2013

M.S., Nuclear Engineering, University of New Mexico, 2015

Abstract

In the solution of the neutron transport equation, the k-effective eigenvalue is related to the average number of neutrons emitted in fission of the system. It can be shown that if the average number of neutrons emitted in fission and the average neutron energy spectrum is conserved, the criticality of a system remains the same without regard to the actual physical fission process. However, the fissioning of a nucleus leads to the emission of any number of neutrons with some probability with correlated emission energies that is a function of the incident neutron energy. In general, Monte Carlo codes used for criticality calculations do not use explicit fission multiplicity sampling instead opting for the expected-value outcome approach. As computational methods and resources advance, there is growing interest in high fidelity modeling, including nuclear fission physics modeling. Extensive criticality benchmarks have been established to verify and validate Monte Carlo calculations versus analytic solutions and benchmarked experiments using the expected-value outcome method and no verification-validation work has been done to date on using explicit fission neutron multiplicity models in MCNP6. To determine the effect

of sampling fission multiplicity probability distributions during criticality (KCODE) calculations, it was necessary to modify MCNP6 to allow for the use of neutron fission multiplicity models during criticality calculations along with correlation of neutron emission energies. Previously, MCNP6 did not allow for the use of these models during criticality calculations and only allowed their use in fixed-source problems. It was found that explicit fission multiplicity sampling agreed within two standard deviations of expected-value outcome sampling calculated k-effective values. Various benchmark suites used to test MCNP6 k-effective criticality calculations demonstrated good agreement using explicit fission multiplicity sampling and confirmed the validity of using explicit fission multiplicity sampling in Monte Carlo criticality calculations.

Contents

List of Figures

List of Tables

Glossary

Ψ	angular neutron flux
$\bar{\nu}$	average number of neutrons emitted in fission event
$\vec{\Omega}$	direction (unit) vector
k_{eff}	effective multiplication factor
E	energy
Σ	macroscopic cross section
σ	microscopic cross section
J	neutron current
$\chi(E)$	neutron fission energy spectra
Q	neutron source
$\hat{e}_S$	normal surface vector
N^k	number density of isotope k
ν	number of neutrons emitted in specific fission event
$\vec{r}$	position vector

P_i	probability of selecting i^{th} isotope, energy, reaction, etc.
ξ	random number
ϕ	scalar neutron flux
$\mathcal{I}^{(n)}$	spectral index for reaction n
S	surface
t	time

Chapter 1

Introduction

A criticality system the ability to sustain a chain reaction by fission neutrons alone in a system. Nuclear criticality is important in determining the critical mass and dimensions of systems such as nuclear reactors, radioactive waste storage containers, and other nuclear systems where criticality is desired or to be prevented. The nuclear criticality of a system can be related to the quantity k_{eff}, the eigenvalue to the neutron transport equation.

Physically, the criticality of a system is determined by the materials and geometry of that system. Material cross sections ultimately determine the number of neutrons produced, lost, scattered, and moderated in a system. Production of neutrons comes primarily from nuclear fission ((n, xn) reactions are usually negligible at the energies of nuclear systems of interest). When a neutron causes fission in a fissionable nucleus, the average number of neutrons emitted in that fission process is a physical constant given the symbol $\bar{\nu}$. $\bar{\nu}$ is a function of the fissioning nucleus and the energy of the incident neutron. By balancing the production and loss of neutrons in a system, a critical configuration of material and geometry can be determined.

In addition to the average number of neutrons emitted in fission, the energies

of these neutrons have impacts on the neutron spectrum of a system. The fission neutron energy emission spectrum $\chi(E \rightarrow E')$ determines the outgoing energy of neutrons and is of importance in the fission process. When multiple neutrons are emitted in a fission event, the correlation of their energies impacts the neutron spectrum. Changes in the neutron spectrum affect the criticality of a system as the energies determine neutron reaction rates in a system.

As computational methods and resources advance, there is growing interest in high fidelity modeling. Approximations and methods used due to limited computational resources and missing nuclear data are being replaced with more physical models and data that better reflect the actual physics. The nuclear fission process is being examined and algorithms and data are being implemented that are closer to the actual physical process are being implemented in codes such as MCNP6 to better reflect the underlying physical processes in neutron transport calculations.

1.1 Calculation of k-Effective for Nuclear Criticality Problems

Monte Carlo methods use random numbers to sample probability distribution functions to create sequences of interaction events for particles in the system. By tracking particles in a system, Monte Carlo methods simulate the behavior of neutrons, photons, and other particles of interest. Monte Carlo methods have been used since the 1960's to determine the criticality of systems [15][16]. For criticality calculations, a power method-like iteration method is used where neutrons produced in one generation are banked for use in the next generation as source particles with sampled directions of emission and emission neutron energy. In Monte Carlo criticality calculations, it is frequently the product of the macroscopic fission cross section Σ_f and

the average number of neutrons emitted in fission ν that is used to determine the number of neutrons emitted in a fission event [8]. The product $\nu\Sigma_f$ is the probability that ν fission neutrons are created per unit path length. However, both the fission macroscopic cross section and the average number of neutrons emitted in fission can be used separately in Monte Carlo calculations. In this thesis, various computational methods used to model nuclear fission process are examined and their impacts on criticality explored:

- In Chapter 2, neutron transport theory and the Monte Carlo methods are introduced.
- In Chapter 3, various sampling methods for fission neutron production are described along with the Lawrence Livermore Fission Library implemented for testing multiplicity sampling.
- In Chapter 4, results for multiplicity sampling are compared with the default expected-value outcome sampling method.
- In Chapter 5, sensitivity theory is used to determine similarity between nuclear systems tested using the various multiplicity sampling techniques.
- In Chapter 6, the uncertainty of $\bar{\nu}$ is determined for various nuclear systems.
- In Chapter 7, the effects of energy correlation of prompt fission neutron energies on k-effective are studied.
- In Chapter 8, conclusions are drawn for the multiplicity sampling methods and energy correlation impacts on k-effective.

Chapter 2

Background

2.1 The Neutron Transport Equation

The neutron transport equation is a balance equation for neutrons in a system. Neutrons undergo a variety of interactions and may be captured, leaked, scattered, or cause a fission which produces more neutrons. The neutron transport equation is a form of the Boltzmann transport equation [14] and is a function of seven variables: three spatial variables, two angular variables, energy, and time.

Inherent in the derivation of the neutron transport equation are some physical assumptions about the system being considered [7]. For the neutron transport equation to be valid, the following must be true: the medium is fixed, neutrons interact only with nuclei and not other neutrons, particle interactions are a Markov process (events only depend on the current state of the system), relativistic effects and outside forces (electric and magnetic fields, gravity, etc.) are neglected, and material properties do not change due to interactions with neutrons. For problems with a fission source of neutrons, the neutron transport equation can be recast into a static eigenvalue problem.

The time-dependent linear Boltzmann transport equation for neutrons with prompt neutron fission and external sources for the angular neutron flux is given as:

$$\frac{1}{v}\frac{\partial\Psi(\vec{r},E,\hat{\Omega},t)}{\partial t}+\hat{\Omega}\cdot\nabla\Psi(\vec{r},E,\hat{\Omega},t)+\Sigma_t\Psi(\vec{r},E,\hat{\Omega},t)\Psi(\vec{r},E,\hat{\Omega},t).=$$
$$Q(\vec{r},E,\hat{\Omega},t)+\iint\Psi(\vec{r},E',\hat{\Omega}',t)\Sigma_s(\vec{r},E'\rightarrow E,\hat{\Omega}\cdot\vec{\Omega}')d\vec{\Omega}'\ dE'$$
$$+\frac{1}{4\pi}\iint\nu\chi(\vec{r},E',E)\Sigma_f\Psi(\vec{r},E',\hat{\Omega}',t)\ d\vec{\Omega}'\ dE' \quad (2.1)$$

Equation 2.1 is a balance equation for neutrons in a system: $Q(\vec{r},E,\hat{\Omega},t)$ is an external source of neutrons, Σ_s,Σ_f, and Σ_t are the scattering, fission, and total macroscopic cross sections are represent losses and gains due to scattering, the fission neutron source, and the total number of collisions in the system respectively. Leakage from the system is described by the term $\hat{\Omega}\cdot\nabla\Psi(\vec{r},E,\hat{\Omega},t)$. The $\chi(\vec{r},E',E)$ represent the energy emission spectrum for neutrons released in fission and is of particular interest in this thesis.

Suitable initial and boundary conditions must be placed on Equation 2.1; for example vacuum, reflected, and periodic boundary conditions. In this work, the systems analyzed allowed for the leakage of neutrons so the following vacuum boundary condition is placed:

$$\Psi(\vec{r},E,\hat{\Omega})=0,\ \text{if}\ \hat{\Omega}\cdot\hat{e}_S<0\ \text{for}\ \vec{r}\ \text{on S}\ , \quad (2.2)$$

where S is the domain surface and $\hat{\Omega}\cdot\hat{e}_S<0$ states that no neutron can reenter the system.

The neutron transport equation can be rewritten in operator form as:

$$\frac{1}{v}\frac{\partial\Psi(\vec{r},E,\hat{\Omega},t)}{\partial t} = Q + \Big[S+M\Big]\Psi - \Big[L+T\Big]\Psi(\vec{r},E,\hat{\Omega},t) \tag{2.3}$$

where Q is the external source, S is the scattering-in source term, M is the fission source, and L and T are losses due to leakage and collisions.

For problems with fission multiplication, the neutron transport equation is rewritten to create a static eigenvalue problem (a steady-state problem). A scaling factor k_{eff} is placed on the multiplication. Setting the time derivative to zero, $\frac{\partial\Psi}{\partial t} = 0$, and introducing the static eigevalue, Equation 2.3 is rewritten as

$$\Big[L+T\Big]\Psi_k(\vec{r},E,\hat{\Omega}) = \Big[S+\frac{1}{k_{\text{eff}}}M\Big]\Psi_k \tag{2.4}$$

where Ψ_k is the steady-state angular flux. The effective multiplication factor k_{eff} scales the fission source and permits a steady state solution. A system is said to be:

Supercritical: $k_{\text{eff}} > 1$ when a system's neutron population grows without bound,

Critical: $k_{\text{eff}} = 1$ when a system's neutron population is constant due to a self-sustaining fission chain reaction,

Subcritical: $k_{\text{eff}} < 1$ when a system's neutron population asymptotically approaches zero.

Other integral parameters such as total leakage and spectral indices are also explored to determine differences between systems when explicit fission multiplicity models and explicit prompt fission neutron energy correlations are implemented in MCNP6. Total leakage is defined as

$$J = \int_S dA \int_0^\infty dE \int_{\hat{\Omega}\cdot\hat{e}_s>0} \hat{\Omega}\cdot\hat{e}_s\psi(\vec{r}_s, E, \hat{\Omega})\ d\hat{\Omega} \tag{2.5}$$

where $\hat{e}_s$ is the unit outward normal vector on the surface of the domain S and $\vec{r}_s$ denotes that the angular flux is evaluated at the surface of the domain. Also of importance are the spectral indices. Spectral indices reflect changes in the neutron energy spectra and can be used to determine the impact of different fission neutron energy correlations. The spectral indices are defined as

$$\mathcal{I}^{(n)}(\vec{r}) = \frac{1}{N}\int_0^\infty dE \int_{4\pi} \Sigma^{(n)}(\vec{r}, E, \hat{\Omega})\psi(\vec{r}, E, \hat{\Omega})\ d\hat{\Omega} \tag{2.6}$$

where $\Sigma^{(n)}(\vec{r}, E, \hat{\Omega})$ is a particular neutron-induced cross section for some isotope n, and N is defined as a similar reaction of a well known quantity such as the fission cross section of uranium-235, $\Sigma_f^{^{235}U}(\vec{r}, E)$.

In this work, spectral indices are with respect to the uranium-235 fission reaction rate, given as

$$N(\vec{r}) = \int_0^\infty dE\Sigma_f^{^{235}U}(\vec{r}, E)\phi(\vec{r}, E) \tag{2.7}$$

where $\phi(\vec{r}, E)$ is the scalar flux defined as the angular flux integrated over all angles in $\hat{\Omega}$,

$$\phi(\vec{r}, E) = \int_{4\pi} d\hat{\Omega}\ \psi(\vec{r}, E, \hat{\Omega}). \tag{2.8}$$

In this work changes in the effective multiplication factor are explored when explicit multiplicity fission models are implemented.

2.2 Monte Carlo Methods for Neutron Transport

The Monte Carlo method for solving the neutron transport equation is well established [5]. It has been used for over 70 years to solve problems in nuclear reactor analysis, finance, shielding and medical imaging, and a host of other problems in different fields. With regards to neutron transport, the Monte Carlo method simulates individual neutron histories using random numbers to generate sequences of events. Monte Carlo allows for the explicit modeling of geometry, materials, and particle interactions using continuous and multigroup nuclear cross section data. As the neutron transport process is a Markov process, as more particle histories are simulated, the average quantities computed approach the true solution of the neutron transport equation. Because of the independent nature of neutron histories, Monte Carlo methods lend themselves immediately to parallelism and can take full advantage of large computational multi-core clusters becoming readily available to researchers.

MCNP6 and Monte Carlo neutral particle transport codes solve the linear Boltzmann Transport Equation for neutrons. Some assumptions are made in the application of Monte Carlo: neutrons are treated as particles, not waves. In addition, neutrons move in a straight line between interactions, and collisions are assumed to occur instantaneously at a point in space. If each neutron history is an independent, identically distributed trial and all neutrons see the same probability densities in all

of the phase space (no change in material properties), the linear transport equation can be solved directly by Monte Carlo.

The actual mechanics of a Monte Carlo calculation are as follows: a source neutron is introduced into a geometric cell with time-independent material properties. The total cross section in a cell is given by

$$\Sigma_t = \sum_k N^k \sigma_t^k \tag{2.9}$$

where N^k and σ_t^k are the number density and microscopic cross section of the k-th material respectively. The distance to interaction for the neutron is a function of the total macroscopic cross section in the cell, and a random number is generated to determine the distance s to the next interaction using the following relation

$$s = \frac{-1}{\Sigma_t} \ln \xi \tag{2.10}$$

where Σ_t is the total macroscopic cross section and ξ is a random number between 0 and 1. The distance to the edge of the geometric cell d is calculated. If s $>$ d the particular is transported to the next cell, and Equation 2.10 is used to determine a new distance to interaction.

In the case where s $<$ d, an interaction takes place within the cell. Using the material cross section data for the cell, an interaction in an isotope J is selected with probability

$$P_J = \frac{N^J \sigma_t^J}{\Sigma_t}. \tag{2.11}$$

Once an isotope has been selected, the reaction type is selected. A reaction σ_J is selected with probability

$$P_J = \frac{\sigma_J}{\sigma_t} \tag{2.12}$$

where σ_t is the total microscopic cross section of the previously selected isotope.

Once a collision isotope and reaction type are selected, a neutron is either absorbed or scattered. In the case of scattering, the exit energy and direction are determined from conservation of energy and momentum and scattering laws, either through models or tabulated data.

If a neutron is absorbed, it may cause a fission if isotope J is fissionable. Secondary particles (neutrons) are created with the number of neutrons emitted in fission determined by various sampling methods. Using power iteration, the criticality of a system can be determined using Monte Carlo. The impacts of two fission number sampling methods, expected-value outcome sampling and explicit fission multiplicity sampling, on k-effective are explored in this thesis.

2.3 Nuclear Fission Multiplicity

In the fissioning of a nucleus, there is a probability of emitting n number of fission neutrons with some probability P_n. This multiplicity distribution is a function of the incoming neutron energy. Traditionally, nuclear data experiments focused exclusively

on determining the average number of neutrons emitted in fission $\bar{\nu}$. However, work on explicit multiplicity distributions has been done and various distributions have been measured for major actinides. It is these distributions that are used in explicit fission multiplicity sampling for criticality calculations. Figures 2.1, 2.2, and 2.3 show the fission multplicity distributions as functions of energy for plutonium-239, uranium-235, and uranium-238 respectively. The expectation value of the fission multiplicity distribution at some energy E is the tabulated $\bar{\nu}$ value found in ACE (ENDF) data files:

$$\bar{\nu}(E) = \sum_{n=0}^{N} \nu_n(E) P_n(E). \tag{2.13}$$

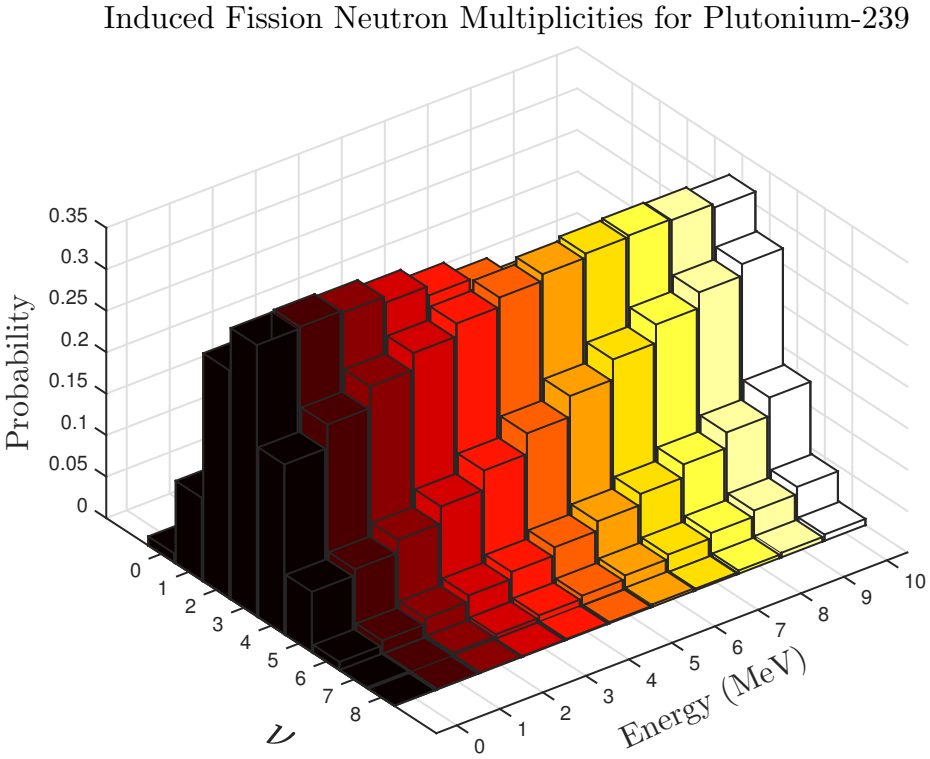

Figure 2.1: Plutonium-239 Fission Multiplicity Distribution

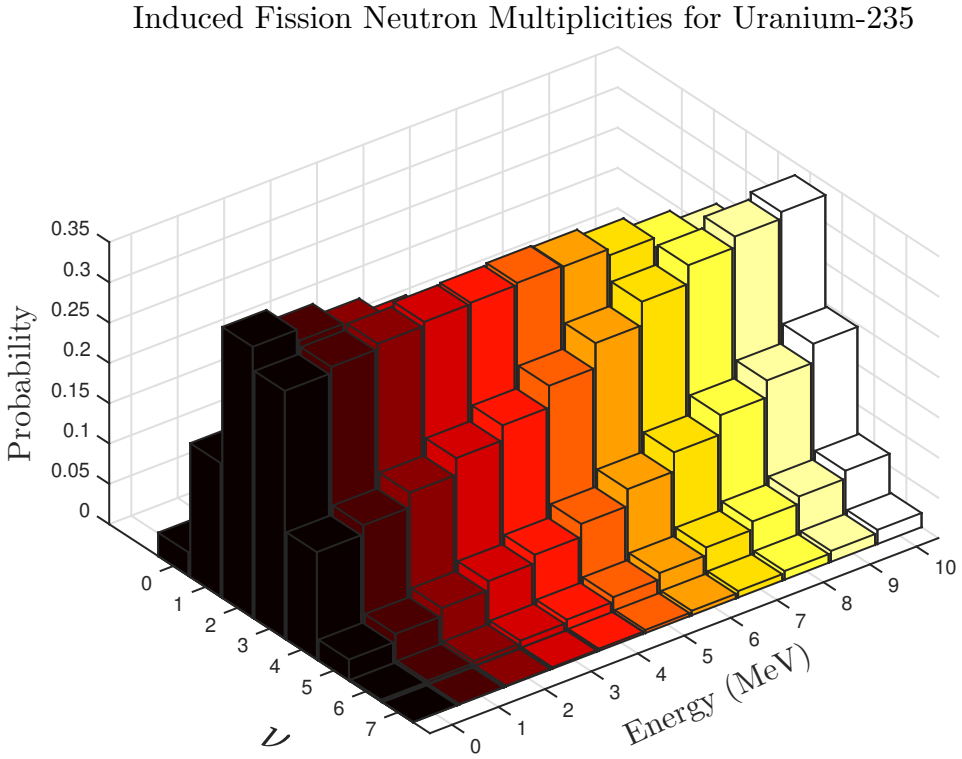

Figure 2.2: Uranium-235 Fission Multiplicity Distribution

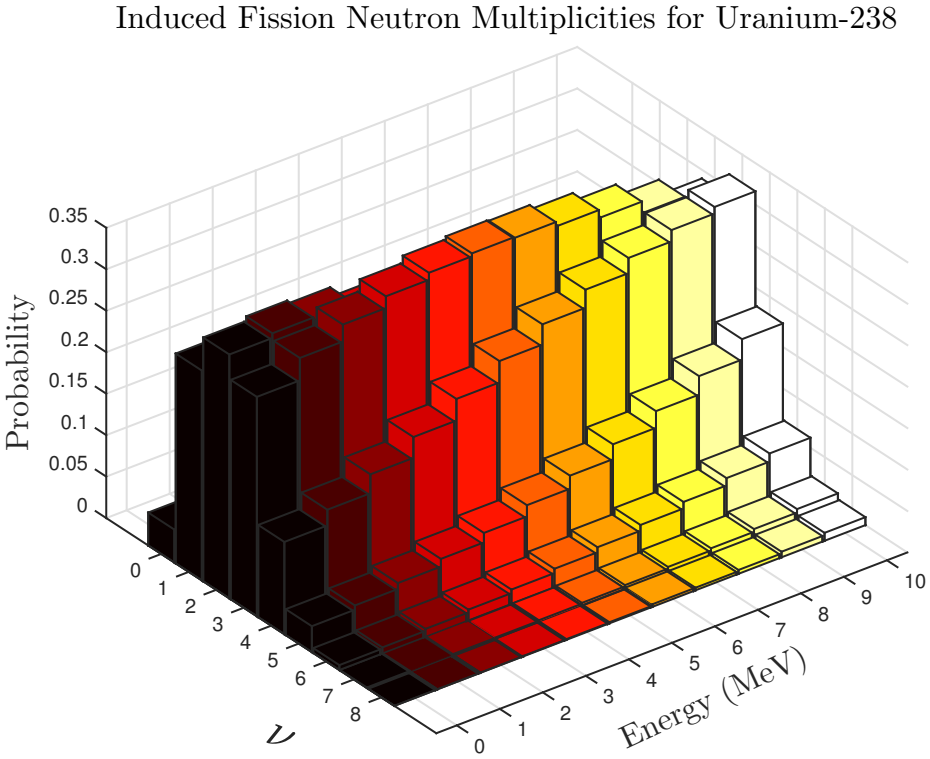

Figure 2.3: Uranium-238 Fission Multiplicity Distribution

Chapter 3

Fission Neutron Multiplicity MCNP6 Criticality: Preliminaries

Historically, Monte Carlo codes have used the expected-value outcome approach to fission neutron production during criticality calculations. Extensive benchmarks have been established to verify and validate Monte Carlo calculations versus experiments using this method and no verification-validation work has been done on using explicit fission neutron multiplicity models in MCNP. To determine the effect of sampling fission multiplicity probability distributions, it was necessary to modify MCNP6 to allow for the use of neutron fission multiplicity models during criticality calculations. Previously, MCNP6 did not allow for the use of these models during criticality ("KCODE") calculations and only allowed their use in fixed-source problems. For the testing of fission neutron multiplicity, MCNP6 was coupled to the Lawrence Livermore National Laboratory (LLNL) Fission Library to sample the emitted number of neutrons per fission. In the following sections the LLNL Fission Library and the benchmark libraries used to test the code are described.

3.1 Expected-Value Outcome Sampling for Fission Events

MCNP6 uses expected-value outcomes for the generation of secondary particles after a fission event. If a collision which results in fission is considered, the expected number of fission neutrons produced per collision is given by

$$\#\text{ of neutrons emitted n} = \text{wgt} \cdot \frac{\nu\Sigma_f}{\Sigma_t} \tag{3.1}$$

where $\nu\Sigma_f$, Σ_t, and wgt are the total number of neutrons emitted per fission macroscopic cross section, the total macroscopic cross section, and the particle weight respectively. To sample the number of neutrons produced in the collision, the following algorithm is used:

Algorithm 1 Calculate ν, number of neutrons produced in fission

If: $r = wgt \cdot \frac{\nu\Sigma_f}{\Sigma_t}, n = int[r]$
Then: Produce $\nu = n$ fission neutrons with probability one and an additional fission neutron with probability $r - n$

As an example, we consider the following expected number of fission neutrons produced per collision:

Let: $r = wgt \cdot \frac{\nu\Sigma_f}{\Sigma_t} = 1.75$, n = int[r] = 1
Generate: Random number $\xi \in [0, 1)$
If: $\xi < 0.75$, then produce $\nu = 2$ neutrons,
Else: Produce $\nu = 1$ neutron
Or:
Produce: $\nu = \text{int}[0.75 + \xi]$ neutrons

Replacing random sampling of an event with an expected-outcome eliminates the

variance for that particular event and implies uncorrelated outcomes for multiple sampled events.

3.2 Fission Neutron Multiplicity Sampling

In this section, we examine the fission neutron multiplicity probability distributions and the sampling methods used in MCNP6.

The probability of emitting an integral number of neutrons ν is given by the probability P_ν which is a function of the distribution of excitation energies to fission fragments [19]. When there is no experimental data, MCNP6 employs Terrell's model of fission neutron multiplicity distributions. In this model, it is assumed that neutrons will be emitted from fission fragments whenever this is energetically possible. Two more simplifying assumptions are made: the emission of any neutron from any fission fragment reduces the excitation of the fission fragment by ΔE and the total excitation energy from two fission fragments from binary fission has a Gaussian or normal distribution.

The cumulative emission probability is shown [19] to be given by

$$\sum_{n=0}^{\nu} P_n(E) = \frac{1}{\sqrt{2\pi}} \int_{-\infty}^{(\nu-\bar{\nu}+\frac{1}{2}+b)/\sigma} e^{\frac{-t^2}{2}} dt \tag{3.2}$$

where $\bar{\nu}$ is the average number of neutrons emitted in fission at that energy and σ and b are experimentally determined values. In this expression, only $\bar{\nu}$ and σ are independent values as b is determined by the condition that

$$\bar{\nu} = \sum_{\nu=0}^{\infty} \nu P_{\nu}. \tag{3.3}$$

In almost all cases, b is found to be $b < 10^{-2}$.

The probability of emitting n neutrons in fission is given by

$$P_0 = \frac{1}{\sqrt{2\pi\sigma^2}} \int_{-\infty}^{1/2} \exp\left(\frac{-(x - \bar{\nu} + b)^2}{2\sigma^2}\right) dx \tag{3.4}$$

and

$$P_{n\neq 0} = \frac{1}{\sqrt{2\pi\sigma^2}} \int_{n-1/2}^{n+1/2} \exp\left(\frac{-(x - \bar{\nu} + b)^2}{2\sigma^2}\right) dx. \tag{3.5}$$

Explicit fission multiplicity modeling in MCNP6 uses experimental data and derived expressions for the calculation of the fission neutron multiplicity. MCNP6 uses measured data for actinide fission when available and uses the expressions by Terrell when there is no data.

When experimental data is available for sampling, a table search is done to determine the number of neutrons emitted in fission. If ξ is a random number on the interval [0,1), then the number of neutrons emitted in a fission $\xi = i$ if

$$P_{i-1} \leq \xi < P_i \tag{3.6}$$

where P_i and P_{i-1} are the cumulative density function for ν equal to i and $i-1$ respectively.

When Terrell's model for fission neutrons is employed, the following algorithm [6] is used to sample the number of neutrons emitted in fission:

Algorithm 2 Calculate ν, number of neutrons produced in fission

Let: w = $\sqrt{2}\sigma$, bshift = -0.43287, Temp1 = $\bar{\nu}$ + 0.5, Temp2 = (Temp1/w)^2
ExpO = e$^{\text{-Temp2}}$, cshift = Temp1 + bshift + ExpO/(1-ExpO)
While: $(\nu < 0)$
Do: r = $\sqrt{-\ln(\xi_1)}$
$\theta = 2\pi\xi_2$
ν = wrcos(θ) + cshift
Return: floor(ν)

Unlike expected-value outcome sampling, variance is introduced through the random sampling of ν, which introduces additional variance in calculated average quantities.

3.3 The Lawrence Livermore National Laboratory Fission Library

The Lawrence Livermore National Laboratory (LLNL) Fission Library is a general purpose software library used to simulate neutron distributions from spontaneous and neutron-induced fission reactions [20]. The LLNL Fission Library incorporates available multiplicity measurements from the literature and uses empirical models when data is not available. The models scale multiplicity data to match the average multiplicity value $\bar{\nu}$ found in the evaluated data libraries.

3.3.1 The LLNL Fission Library in MCNP6

Neutron-induced fission data in the LLNL Fission Library can be specified using the internal option (`nudist`). This internal option determines the methods used for parametrizing multiplicity data and renormalizing overall distributions to agree with specific measurements of $\bar{\nu}$. The LLNL Fission Library used during MCNP6 calculations is the default option (`nudist = 3`). During a fission reaction, the incident neutron energy E_n is used to determine the multiplicity probability distribution function P_ν. P_ν data is obtained from the multiplicity distributions in Gwin, Spencer, and Ingle [9] and from [11]Zucker and Holden[22]. The multiplicity probability distribution function is chosen using the $\bar{\nu}$ at the neutron incident energy E_n for the given fission event. To explain, we use the example presented by Verbeke [20]. Consider a $\bar{\nu}$ of 2.45 at the energy of the incident neutron. If there are two probability distribution functions, P_ν(1 MeV) and P_ν(2 MeV) with $\bar{\nu}$ equal to 2.4 and 2.6, respectively, the probability of sampling the number of neutrons ν from P_ν(1 MeV) and P_ν(2 MeV) will be 75% and 25%, respectively. If the $\bar{\nu}$ is not in the range of average emitted fission neutrons in the tabulated data or there is no explicit multiplicity data available, the LLNL Fission Library uses Terrell's approximation with the width of the distribution σ set to 1.079 and the correction factor b set to less than 0.01 [19].

3.3.2 Prompt Fission Neutron Spectra and Neutron Energy Correlations

All fission neutron energy spectra (both spontaneous and induced) are modeled using an analytical Watt spectrum found in the Evaluated Nuclear Data Library, ENDL [12]. The Watt spectrum is given by

$$W(a,b,E') = Ce^{-aE'}\sinh(\sqrt{bE'}) \tag{3.7}$$

where

$$C = \sqrt{\pi\frac{b}{4a}}\frac{e^{\frac{b}{4a}}}{a}, \tag{3.8}$$

and E' is the secondary energy neutron. The coefficients a and b vary weakly for each fissile isotope considered. For the case of neutron-induced fission, parameter b is set equal to 1.0 and parameter a is given as a quadratic function of incident neutron energy:

$$a(E) = a_0 + a_1E + a_2E^2 \tag{3.9}$$

where the coefficients $a_0, a_1,$ and $, a_2$ are given for 40 isotopes.

For multiplicity sampling enabled criticality calculations, the LLNL Fission Library was compiled using the default neutron energy conservation correlation (`correlation = 0`). For a single fission event, neutron energies are sampled independently from the material prompt fission neutron spectrum, and there is no explicit energy conservation.

3.3.3 Fission Neutron Emission Spectra Differences Between LLNL Fission Library and MCNP6

The LLNL Fission Library assumes that all fissile isotopes' neutron emission energy spectra follows the same functional form as described in the previous section. MCNP6 however uses ENDF models to describe fission neutron spectra with this data found in each of the fissile isotopes ACE data files. Of particular importance is the Simple Maxwellian Fission Spectrum model. Major actinides like uranium-235 and Plutonium-239 fission neutron spectra are described by the following form:

$$f(E \to E') = \frac{\sqrt{E'}}{I} e^{-E'/\theta(E)} \tag{3.10}$$

where E' is in the emitted neutron energy, $\theta(E)$ is the temperature, and I is a normalization condition defined as

$$I = \theta^{3/2}\left[\frac{\sqrt{\pi}}{2}\,\mathrm{erf}(\sqrt{(E-U)/\theta}) - \sqrt{(E-U)/\theta}\exp\left(-(E-U)/\theta\right)\right] \tag{3.11}$$

where E is the incident neutron energy and U is a constant that defined the upper energy limit for the neutron emitted so that $0 \leq E' \leq E - U$ in the LAB frame.

3.4 The MCNP Criticality Validation Suite

To compare MCNP6 multiplicity-enabled sampling for criticality calculations to the default expected-value outcome approach for fission neutron production, two suites of criticality cases were chosen as benchmarks. Two suites (MCNP 31 ICSBEP

Case Criticality Validation Suite and the MCNP Extended ICSBEP Case Cricality Validation Suite) , included in all MCNP6 installations, were chosen.

3.4.1 The MCNP 31 ICSBEP Case Criticality Validation Suite

Preliminary benchmarking was done using the MCNP Criticality Validation Suite included with all MCNP6 installations. The MCNP Criticality Validation Suite consists of 31 benchmarks taken from the International Handbook of Evaluation Criticality Safety Benchmark Experiments (ICSBEP) [3]. The 31 benchmarks include simulations of fast, intermediate, and thermal spectrum problems, reflected (light and heavy reflectors) and non-reflected problems, as well as fuel lattice and liquid solution problems. Descriptions of the 31 cases are taken directly from the Testing/VALIDATION_CRITICALITY directory README file found in all MCNP6 installations and can be seen in Table 3.1.

3.4.2 The MCNP Extended ICSBEP Case Criticality Validation Suite

Additional validation of explicit multiplicity sampling was done using the MCNP Extended Criticality Validation Suite. The suite consists of 119 ICSBEP benchmarks. The suite contains thermal, intermediate, and fast spectrum benchmarks as well as metal, mixed, and solution systems. The validation suite consists of low enriched uranium, intermediate enriched uranium, high enrichment uranium, uranium-233, and plutonium benchmarks. Table 3.2 details the benchmarks found in the suite and their composition, spectrum, and isotopes.

Case	Spectrum	ICSBEP	Description
Jezebel-233	Fast	U233-MET-FAST-001	Bare sphere of 233U
Flattop-23	Fast	U233-MET-FAST-006	Sphere of 233U reflected by normal U
U233-MF-05	Fast	U233-MET-FAST-005, c2	Sphere of 233U reflected by beryllium
Falstaff-1	Intmed	U233-SOL-INTER-001, c1	Sphere of uranyl flouride solution enriched in 233U
SB-2 1/2	Thermal	U233-COMP-THERM-001, c3	Lattice of 233U fuel pins in water
ORNL-11	Thermal	U233-SOL-THERM-008	Large sphere of uranyl nitrate solution enriched in 233U
Godiva	Fast	HEU-MET-FAST-001	Bare HEU sphere
Tinkertoy-2	Fast	HEU-MET-FAST-026, cC-11	3 x 3 x 3 array of HEY cylinders in paraffin box
Flattop-25	Fast	HEU-MET-FAST-028	HEU sphere reflected by normal U
Godiver	Fast	HEU-MET-FAST-004	HEU sphere reflected by water
Zeus-2	Intmed	HEU-MET-INTER-006, c2	HEU platters moderated by graphite and reflected by copper
UH3	Intmed	HEU-COMP-THERM-003, c6	UH3 cylinders reflected by depleted uranium
SB-5	Thermal	U233-COMP-THERM-001, c6	Lattice of HEU fuel pins in water, with blanket of ThO2 pin
ORNL-10	Thermal	HEU-SOL-THERM-032	Large sphere of HEU nitrate solution
IEU-MF-03	Fast	IEU-MET-FAST-003	Bare sphere of IEU (36 wt.%)
BIG TEN	Fast	IEU-MET-FAST-007	Cylinder of IEU (10 wt.%) reflected by normal uranium
IEU-MF-04	Fast	IEU-MET-FAST-004	Sphere of IEU (36 wt.%) reflected by graphite
Zebra-8H	Intmed	MIX-MET-FAST-008, c7	IEU (37.5 wt. %) reflected by normal U and steel
IEU-CT-02	Thermal	IEU-COMP-THERM-002, c3	Lattice of IEU (17 wt. %) fuel rods in water
STACY-36	Thermal	LEU-SOL-THERM-007, c36	Cylinder of IEU (9.97 wt.%) uranyl flouride solution
B&W XI-2	Thermal	LEU-COMP-THERM-008, c2	Large lattice of LEU (2.46 wt.%) fuel pins in borated water
LEU-ST-02	Thermal	LEU-SOL-THERM-002, c2	Sphere of LEU (4.9 wt.%) uranyl fluoride solution
Jezebel	Fast	PU-MET-FAST-001	Bare sphere of plutonium
Jezebel-240	Fast	PU-MET-FAST-002	Bare sphere of plutonium (20.1 at.% 240Pu)
Pu Buttons	Fast	PU-MET-FAST-003, c103	3 x 3 x 3 array of small cylinders of plutonium
Flattop-Pu	Fast	PU-MET-FAST-006	Plutonium sphere reflected by normal U
THOR	Fast	PU-MET-FAST-006	Plutonium sphere reflected by thorium
PU-MF-11	Fast	PU-MET-FAST-011	Plutonium sphere reflected by water
HISS/HPG	Intmed	PU-COMP-INTER-001	Infinite, homog. mixture of plutonium, hydrogen, & graphite
PNL-33	Thermal	MIX-COMP-THERM-002, c4	Lattice of mixed-oxide fuel pins in borated water
PNL-2	Thermal	PU-SOL-THERM-021, c3	Sphere of plutonium nitrate solution

Table 3.1: MCNP Criticality Validation Suite Benchmark Descriptions

LEU		
leu-comp-therm-008-case-1	leu-comp-therm-008-case-2	leu-comp-therm-008-case-5
leu-comp-therm-008-case-7	leu-comp-therm-008-case-8	leu-comp-therm-008-case-11
leu-sol-therm-002-case-1	leu-sol-therm-002-case-2	
IEU		
ieu-met-fast-003-case-2	ieu-met-fast-005-case-2	ieu-met-fast-006-case-2
ieu-met-fast-004-case-2	ieu-met-fast-001-case-1	ieu-met-fast-001-case-2
ieu-met-fast-001-case-3	ieu-met-fast-001-case-4	ieu-met-fast-002
ieu-met-fast-007-case-4	mix-met-fast-008-case-7	ieu-comp-therm-002-case-3
leu-sol-therm-007-case-14	leu-sol-therm-007-case-30	leu-sol-therm-007-case-32
leu-sol-therm-007-case-36	leu-sol-therm-007-case-49	
HEU		
heu-met-fast-001	heu-met-fast-008	heu-met-fast-018-case-2
heu-met-fast-003-case-1	heu-met-fast-003-case-2	heu-met-fast-003-case-3
heu-met-fast-003-case-4	heu-met-fast-003-case-5	heu-met-fast-003-case-6
heu-met-fast-003-case-7	heu-met-fast-028	heu-met-fast-014
heu-met-fast-003-case-8	heu-met-fast-003-case-9	heu-met-fast-003-case-10
heu-met-fast-003-case-11	heu-met-fast-003-case-12	heu-met-fast-013
U233		
u233-met-fast-001	u233-met-fast-002-case-1	u233-met-fast-002-case-2
u233-met-fast-003-case-1	u233-met-fast-003-case-2	u233-met-fast-006
u233-met-fast-004-case-1	u233-met-fast-004-case-2	u233-met-fast-005-case-1
u233-met-fast-005-case-2	u233-sol-inter-001-case-1	u233-comp-therm-001-case-3
u233-sol-therm-001-case-1	u233-sol-therm-001-case-2	u233-sol-therm-001-case-3
u233-sol-therm-001-case-4	u233-sol-therm-001-case-5	u233-sol-therm-008
PU		
pu-met-fast-001	pu-met-fast-002	pu-met-fast-022-case-2
mix-met-fast-001	mix-met-fast-003	pu-met-fast-006
pu-met-fast-010	pu-met-fast-020	pu-met-fast-008-case-2
pu-met-fast-005	pu-met-fast-025-case-2	pu-met-fast-026-case-2
pu-met-fast-009	pu-met-fast-023-case-2	pu-met-fast-018
pu-met-fast-019	pu-met-fast-024-case-2	pu-met-fast-011

Table 3.2: Extended Criticality Validation Input Files

Chapter 4

Fission Neutron Multiplicity MCNP6 Criticality: Validation Results

Initial testing of explicit multiplicity sampling in MCNP6 criticality calculations was done using the MCNP Criticality Validation Suite previously described. The benchmark suite was ran using a Mac executable compiled using the Intel Fortran and GCC compilers. The MCNP Criticality Validation Suite was ran on a late 2013, 16 GB RAM, 2.3 GHz Intel Core i7 processor MacBook Pro. k-effective agreement and differences are discussed in the following chapter.

4.1 Testing Methodology

A modified MCNP6 installation was used to test multiplicity sampling during KCODE calculations. The MCNP Criticality Validation Suite Benchmark was ran using a modified MCNP6 installation initially using the expected-value outcome

method for neutron fission production. The same validation suite was ran using the modified multiplicity-enabled MCNP6 installation using option `FMULT=1`. The `FMULT=1` option allows MCNP6 to sample LLNL Fission Library fissile isotope multiplicity data but not fission neutron energy spectra. Finally, the criticality validation suite was ran using option `FMULT=2` which allowed for sampling of both multiplicity and fission spectrum data from the LLNL Fission Library. Input files were ran using 50000 neutrons per cycle for 250 cycles, with the first 50 cycles skipped. Input files were unmodified except for options enabling multiplicity sampling.

k-effective values and standard deviations for all cases were plotted. Agreement between the two sampling methods was defined as an explicit multiplicity sampling k-effective within two standard deviations of the expected-value outcome k-effective.

4.2 k_{eff} Results for MCNP6 Criticality Validation Suite: Explicit Fission Multiplicity Sampling

The MCNP6 Criticality Benchmark was run for both the default MCNP6 expected-value outcome approach and explicit fission multiplicity sampling. The results were then compared to each other. Initially, 5000 neutrons per cycle were used, with the first 50 cycles skipped and 250 total cycles. Figure 4.2 shows that most cases agree to within two standard deviations (error bars represent 2σ standard deviation for explicit-multiplicity sampling values) of the expected-value outcome k-effective.

The added sampling of fission multiplicity distributions increased the variance of the calculated k-effective for the benchmark cases. It was necessary to increase the number of neutrons per cycle to reduce the variance in calculated k-effective values. 50000 neutrons for 250 total cycles with 50 cycles skipped were run for all benchmark cases to reduce k-effective variance to the same magnitude as expected-

value outcome calcuated k-effectives. Figure 4.2 shows continued agreement within two standard deviations of the expected-value outcome k-effective. The root-mean square deviation for the MCNP6 Criticality Benchmark was found to be 0.0380% as seen in Table 4.1. k-effective values for both sampling schemes and their difference are listed in Table 4.2 along with their difference in $\bar{\nu}$.

Table 4.1: Root-mean-square Deviation for MCNP6 Criticality Benchmark

MCNP6 Criticality Benchmark	
Root-mean-square deviation	0.0380%

Case	Explicit Fission Multiplicity Sampling	Expected-Value Outcome Sampling	Δk	$\Delta\bar{\nu}$
JEZ233	0.9998 ± 0.0002	1.0001 ± 0.0002	-0.0003 ± 0.0003	0.0080
FLAT23	0.9990 ± 0.0003	0.9983 ± 0.0002	0.0007 ± 0.0004	0.0070
UMF5C2	0.9953 ± 0.0002	0.9953 ± 0.0002	0.0000 ± 0.0003	0.0020
FLSTF1	0.9857 ± 0.0003	0.9856 ± 0.0004	0.0001 ± 0.0005	-0.0020
SB25	1.0014 ± 0.0004	1.0012 ± 0.0003	0.0002 ± 0.0005	-0.0020
ORNL11	1.0015 ± 0.0003	1.0015 ± 0.0001	0.0000 ± 0.0003	-0.0010
GODIVA	0.9998 ± 0.0002	1.0000 ± 0.0002	-0.0002 ± 0.0003	0.0070
TT2C11	1.0000 ± 0.0003	1.0006 ± 0.0002	-0.0006 ± 0.0004	0.0050
FLAT25	1.0024 ± 0.0003	1.0031 ± 0.0002	-0.0007 ± 0.0004	0.0050
GODIVR	1.0006 ± 0.0003	1.0001 ± 0.0003	0.0005 ± 0.0004	0.0100
UH3C6	0.9953 ± 0.0003	0.9952 ± 0.0003	0.0001 ± 0.0004	0.0040
ZEUS2	0.9960 ± 0.0003	0.9965 ± 0.0002	-0.0005 ± 0.0004	-0.0060
SB5RN3	0.9955 ± 0.0003	0.9960 ± 0.0003	-0.0005 ± 0.0004	-0.0010
ORNL10	0.9991 ± 0.0003	0.9991 ± 0.0001	0.0000 ± 0.0003	-0.0010
IMF03	1.0030 ± 0.0003	1.0026 ± 0.0002	0.0004 ± 0.0004	0.0010
BIGTEN	0.9940 ± 0.0002	0.9948 ± 0.0002	-0.0008 ± 0.0003	0.0030
IMF04	1.0077 ± 0.0003	1.0075 ± 0.0002	0.0002 ± 0.0004	0.0050
ZEBR8H	1.0192 ± 0.0002	1.0190 ± 0.0001	0.0002 ± 0.0002	-0.0020
ICT2C3	1.0042 ± 0.0003	1.0040 ± 0.0003	0.0002 ± 0.0004	0.0030
STACY3	0.9992 ± 0.0003	0.9989 ± 0.0002	0.0003 ± 0.0004	0.0070
BAWXI2	1.0006 ± 0.0003	1.0007 ± 0.0002	-0.0001 ± 0.0004	-0.0070
LST2C2	0.9956 ± 0.0003	0.9961 ± 0.0002	-0.0005 ± 0.0004	0.0000
JEZPU	0.9993 ± 0.0002	0.9996 ± 0.0002	-0.0003 ± 0.0003	0.0170
JEZ240	1.0001 ± 0.0002	0.9999 ± 0.0002	0.0002 ± 0.0003	0.0080
PUBTNS	0.9991 ± 0.0003	0.9989 ± 0.0002	0.0002 ± 0.0004	0.0160
FLATPU	1.0000 ± 0.0003	0.9998 ± 0.0002	0.0002 ± 0.0004	0.0060
THOR	0.9982 ± 0.0002	0.9979 ± 0.0002	0.0003 ± 0.0003	0.0060
PUSH2O	1.0000 ± 0.0003	1.0002 ± 0.0002	-0.0002 ± 0.0004	0.0080
HISHPG	1.0117 ± 0.0002	1.0117 ± 0.0002	0.0000 ± 0.0003	0.0060
PNL2	1.0038 ± 0.0003	1.0041 ± 0.0003	-0.0003 ± 0.0004	0.0010
PNL33	1.0070 ± 0.0003	1.0063 ± 0.0002	0.0007 ± 0.0004	-0.0060

Table 4.2: MCNP6 Explicit Multiplicity Enabled KCODE Comparisons

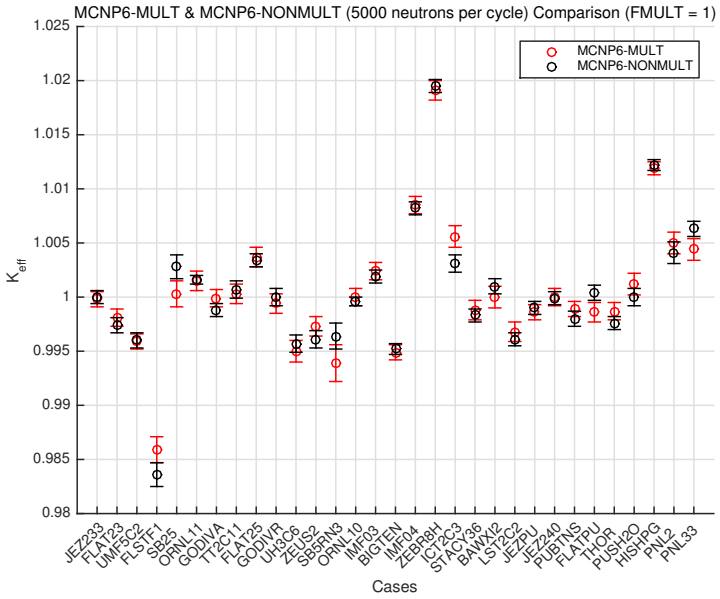

Figure 4.1: Initial Comparison of MCNP6 Fission Number Multiplicity

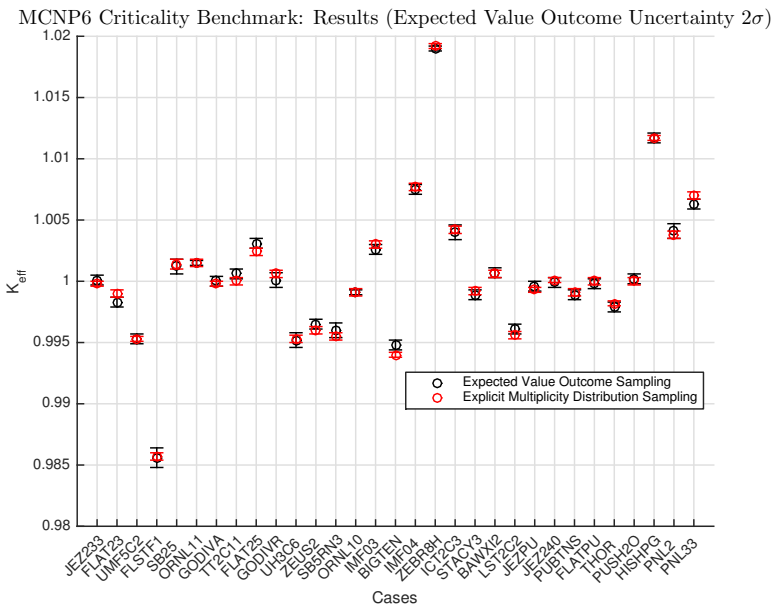

Figure 4.2: Increased Number of Particles Per Cycle-Initial MCNP6 Multiplicity Sampling Testing

4.3 k_{eff} Results for MCNP6 Criticality Validation Suite: Explicit Fission Multiplicity & Fission Neutron Spectra Sampling

k_{eff} results for explicit fission multiplicity sampling with ACE and ENDL fission neutron energy spectra were compared. The root-mean-square deviation was found to be 0.0691% as seen in Table 4.3. Increased disagreement was obtained between the cases, primarily due to differences in the neutron fission spectrum between ACE and ENDL data. Figure 4.3 demonstrates decreased agreement between explicit fission multiplicity sampling with ENDL fission spectra and the expected-value outcome sampling.

Table 4.3: RMS Deviation for MCNP6 Criticality Benchmark-ENDL Fission Spectra

MCNP6 Criticality Benchmark	
Root-mean-square deviation	0.0691%

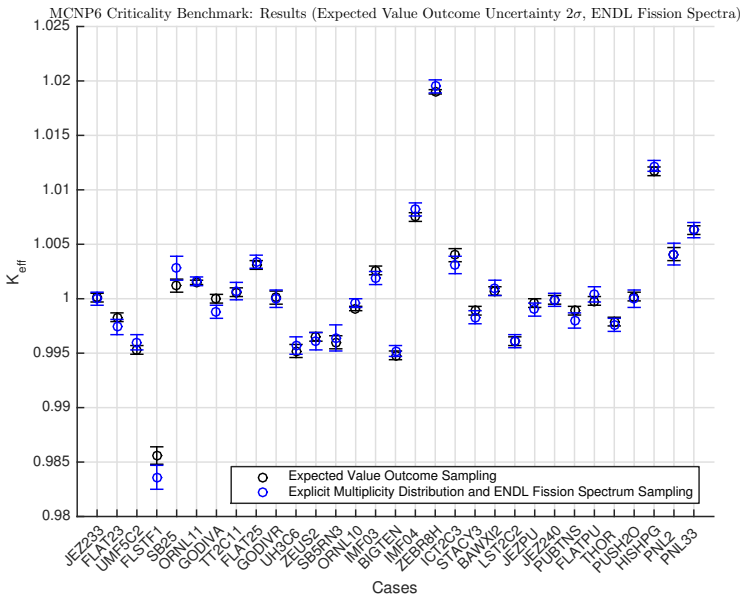

Figure 4.3: k-effective Comparisons Between ACE and ENDL Spectra Data

4.4 k_{eff} Results for MCNP6 Extended Criticality Validation Suite: Explicit Fission Multiplicity Sampling

With initial agreement of the sampling methods for the MCNP6 Criticality Benchmark Suite, the sampling method was tested using the MCNP6 Extended Criticality Benchmark Suite. The suite was subdivided into five categories: PU, HEU, IEU, LEU, and U233. The benchmark was run on the Los Alamos National Laboratory cluster Mapache using 10000 neutrons per cycle for 600 cycles, with the first 100 cycles skipped. Overall agreement (within 2σ of expected-outcome value sampling k-effective) was found for 91 out of the 119 cases.

4.4.1 k_{eff} Results for MCNP6 Extended Criticality Validation Suite: Plutonium Systems

Agreement for plutonium cases was found for 27 of 36 cases. The RMS for the cases was found to be 0.0608%. Cases that were not within two standard deviations of expected-outcome value sampling were a mixture of fast metal systems and thermal solution systems.

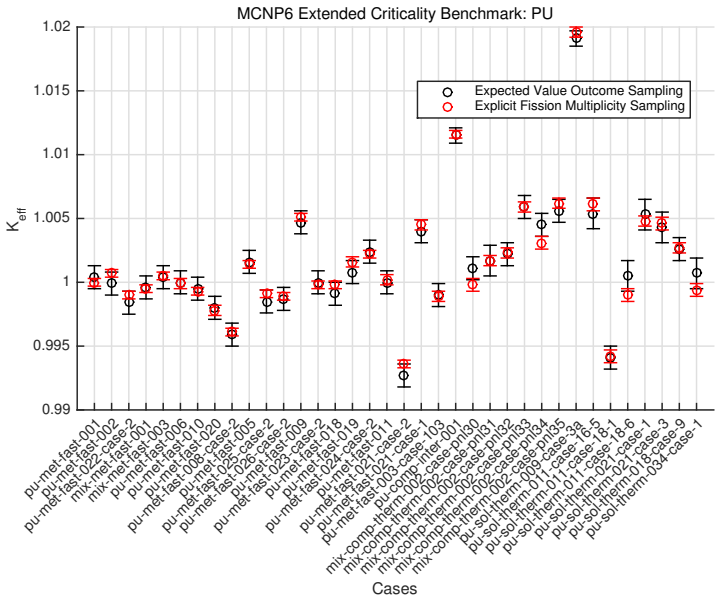

Figure 4.4: k-effective Comparisons for Plutonium Systems

4.4.2 k_{eff} Results for MCNP6 Extended Criticality Validation Suite: High-Enrichment Uranium Systems

Agreement for high-enrichment uranium systems was found for 33 of 40 cases. The RMS for the HEU benchmark portion was found to be 0.0529%. Cases that were not within two standard deviations were found to be primarily metal systems in the fast

and intermediate neutron energy spectra regions with two thermal solution systems.

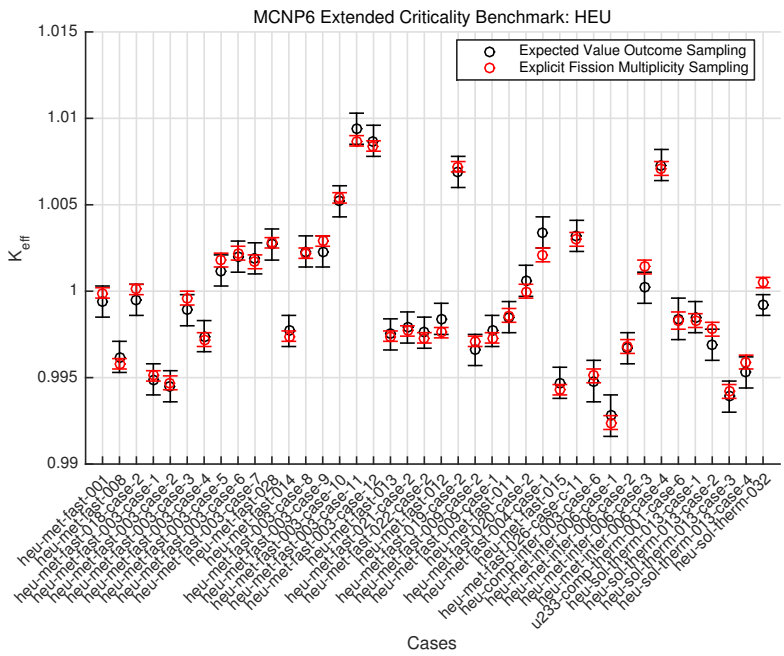

Figure 4.5: k-effective Comparisons for HEU Systems

4.4.3 k_{eff} Results for MCNP6 Extended Criticality Validation Suite: Intermediate Enrichment Uranium Systems

Agreement for intermediate-enrichment uranium systems was found for 11 of 17 cases. The RMS for the IEU benchmark was found to be 0.0587%. Cases that were not found within the two standard deviations were some fast metal and thermal solution systems.

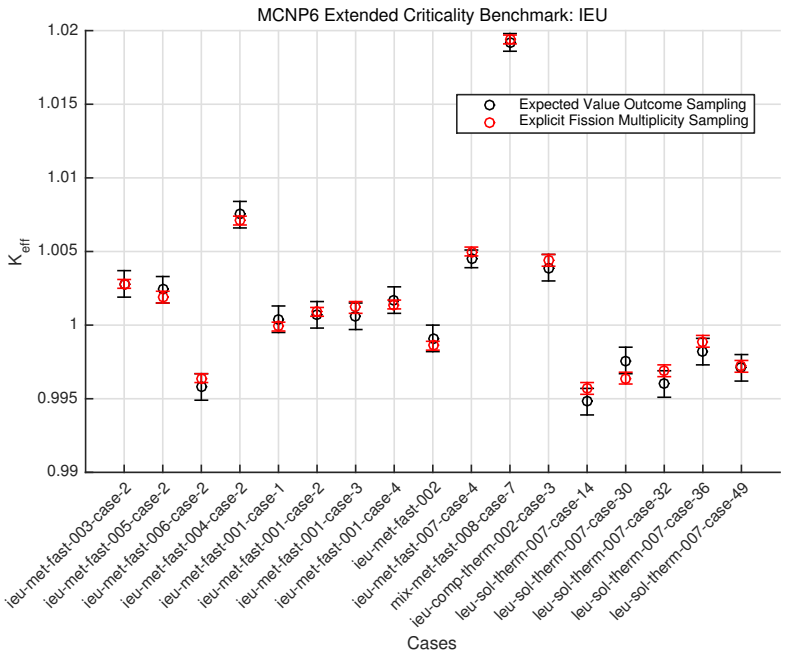

Figure 4.6: k-effective Comparisons for IEU Systems

4.4.4 k_{eff} Results for MCNP6 Extended Criticality Validation Suite: Low Enrichment Uranium Systems

Agreement for low-enrichment uranium systems was found for five of eight cases. The RMS deviation was found to be 0.0717% for the IEU benchmark. In this particular case, all three cases found in disagreement were thermal systems. Two cases were liquid solution systems while the other was a mixed composition system.

4.4.5 k_{eff} Results for MCNP6 Extended Criticality Validation Suite: Uranium-233 Systems

Agreement for uranium-233 systems was found for 15 of 18 cases. The RMS deviation was determined to be 0.0538% for uranium-233 systems. The three cases that were

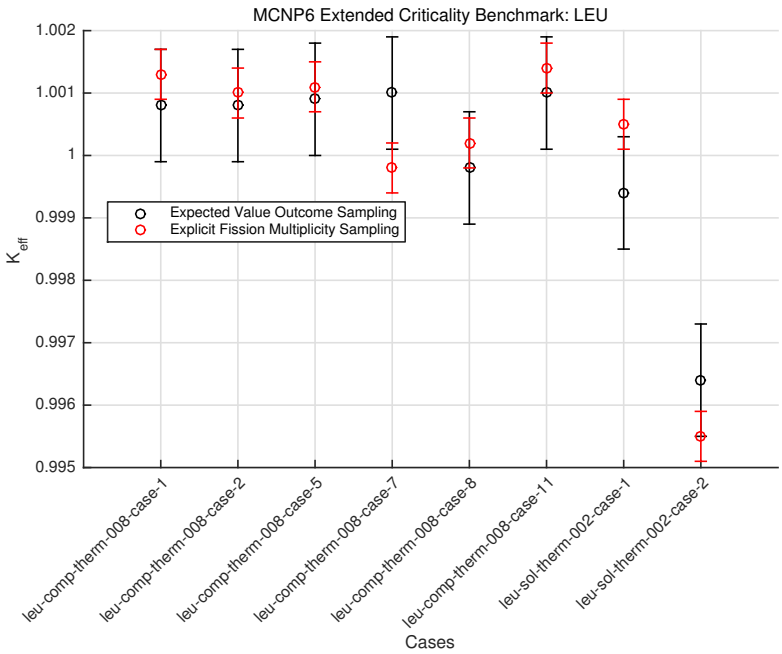

Figure 4.7: k-effective Comparisons for LEU Systems

found to be in disagreement were one fast metal system and two thermal solution systems.

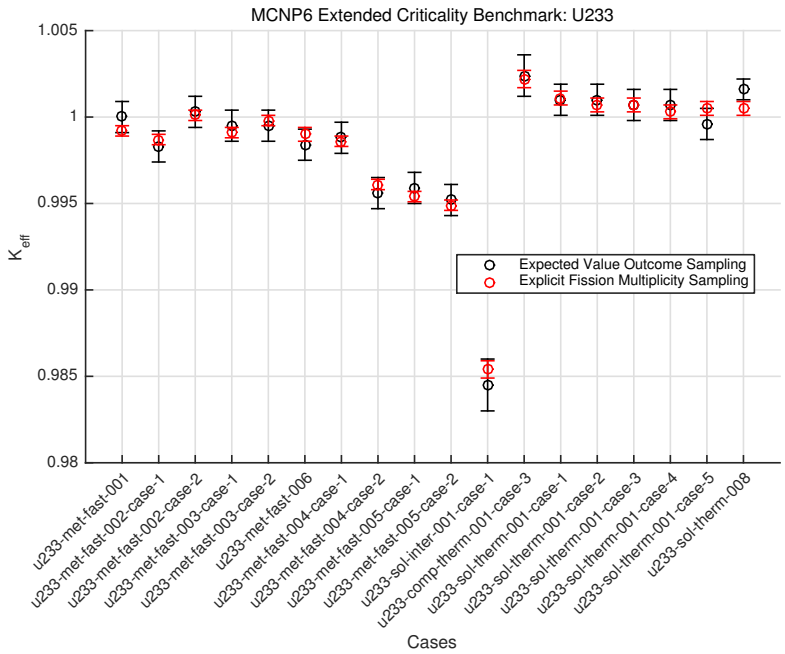

Figure 4.8: k-effective Comparisons for U233 Systems

4.5 k_{eff} Results for MCNP6 Extended Criticality Validation: Fission Multiplicity and Neutron Energy Spectra Sampling

Similar to the MCNP6 Criticality Benchmark Suite, k-effective comparisons were made between the expected-value outcome sampling and fission multiplicity and neutron fission energy sampling approaches. Similar to previous runs, the benchmark was run on the Los Alamos National Laboratory cluster Mapache using ten thousand neutrons per cycle for six hundred cycles with the first one hundred cycles skipped. Agreement was found for only 19 of 119 cases. Testing of LLNL Fission Library prompt neutron fission spectra was done to determine the impact of using another set of data in criticality calculations. The differences in the ENDL and ACE fission

neutron energy spectra described in Section 3.3.3 caused substantial differences in calculated k-effective values. For this reason, it is not recommended to use ENDL fission spectra data in MCNP6 criticality calculations.

4.5.1 k_{eff} Results for MCNP6 Extended Criticality Validation Suite-ENDL Fission Spectra Sampling: Plutonium Systems

One case of 36 was found to be in agreement as seen in Table 4.9 for plutonium systems. Plutonium isotopes' fission neutron energy spectra are given by a Simple Maxwellian distribution in ENDF data evaluations as described in Section 3.3.3. ENDL fission spectra for plutonium isotopes are given by a Watt spectrum. No agreement was expected and k-effective comparisons support this conclusion. The RMS deviation was found to be 0.6759%.

4.5.2 k_{eff} Results for MCNP6 Criticality Validation-ENDL Fission Spectra Sampling: High-Enrichment Uranium Systems

Eleven of 40 cases were found to be in agreement for HEU systems as seen in Table 4.10. Similar to plutonium, some uranium isotopes' fission neutron energy spectra are represented by a Simple Maxwellian distribution. The RMS deviation was found to be 0.4304%. Thermal systems show the greatest differences in k-effective, suggesting changes in k-effective are due to changes in the average energy of a neutron causing fission in the system.

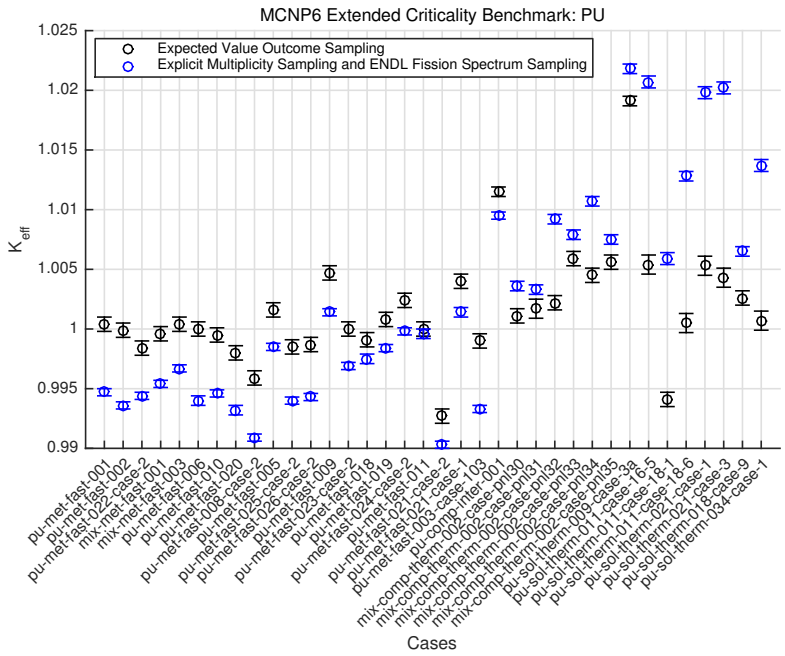

Figure 4.9: k-effective Comparisons with ENDL Fission Spectra Sampling for Plutonium Systems

4.5.3 k_{eff} Results for MCNP6 Criticality Validation-ENDL Fission Spectra Sampling: Intermediate Enrichment Uranium Systems

No cases of 17 were found to be in agreement for IEU systems. k-effectives were found to disagree by three standard deviations in almost all cases as can be seen in Table 4.11. In all thermal spectrum cases, the k-effective of explicit multiplicity and ENDL spectra sampling was found to be greater than the expected-value outcome k-effective. The RMS deviation was calculated as 0.6852%.

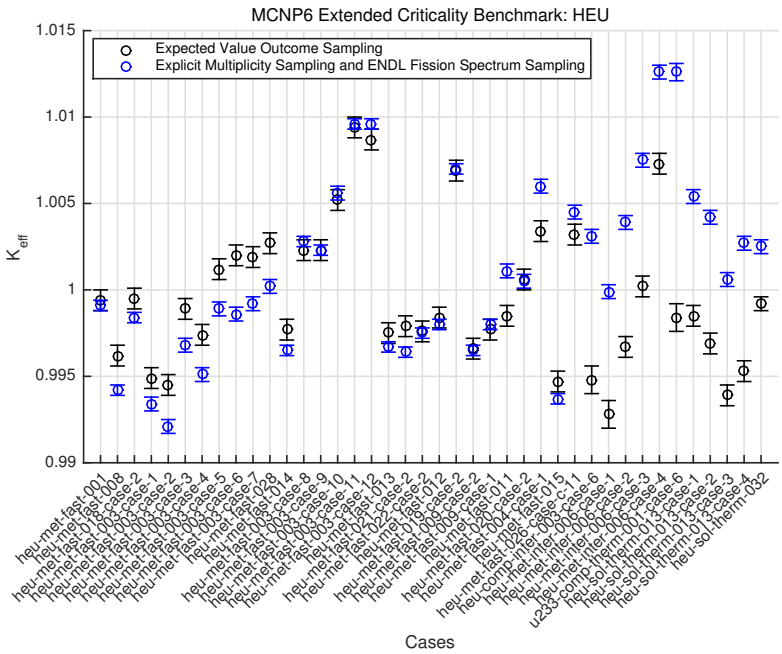

Figure 4.10: k-effective Comparisons with ENDL Fission Spectra Sampling for HEU Systems

4.5.4 k_{eff} Results for MCNP6 Criticality Validation-ENDL Fission Spectra Sampling: Low-Enrichment Uranium Systems

Two of eight cases were found to be in agreement for LEU systems. Thermal solution systems showed the most disagreement as seen in Figure 4.12. The RMS deviation was found to be 0.2763%. Thermal solution k-effective differences imply differences in the thermal fission cross section for uranium isotopes due to differences in the ENDF and ENDL evaluations as expected.

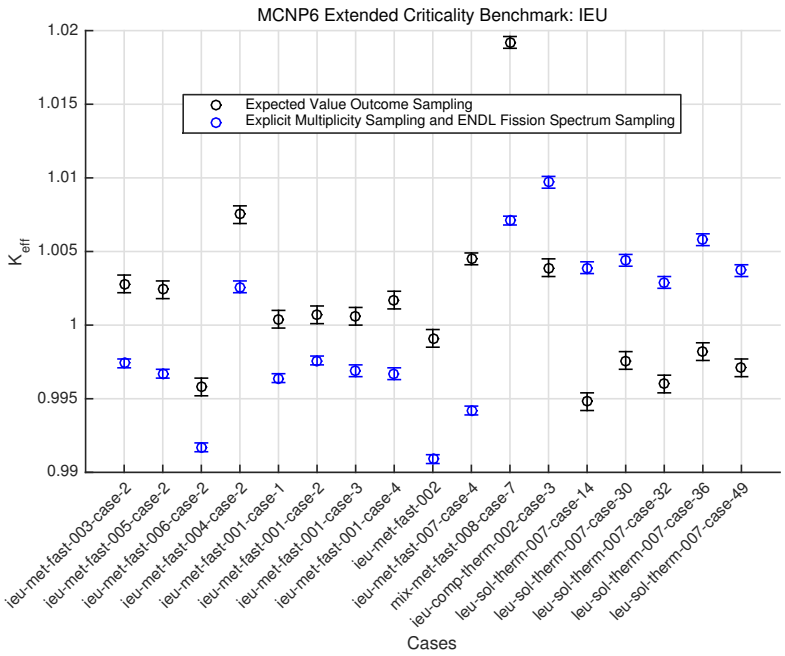

Figure 4.11: k-effective Comparisons with ENDL Fission Spectra Sampling for IEU Systems

4.5.5 k_{eff} Results for MCNP6 Criticality Validationf with ENDL Fission Spectra Sampling: Uranium-233 Systems

Six of 18 uranium-233 systems were found to be in agreement. In particular, fast metal uranium systems agreed relatively well as seen in Figure 4.13. However, thermal solution uranium-233 systems were found to be in substantial disagreement (3σ). The sole intermediate neutron spectrum case was found to differ by Δk of approximately 0.02. The RMS deviation was found to be 0.8797%, primarily driven by differences in k-effective of thermal spectra, solution-based, uranium-233 systems.

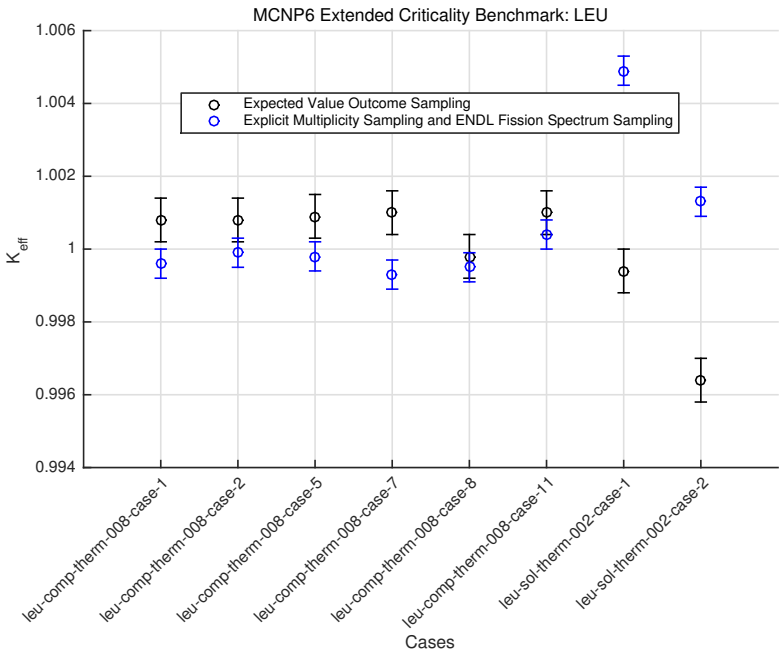

Figure 4.12: k-effective Comparisons-ENDL Fission Spectra Sampling for LEU Systems

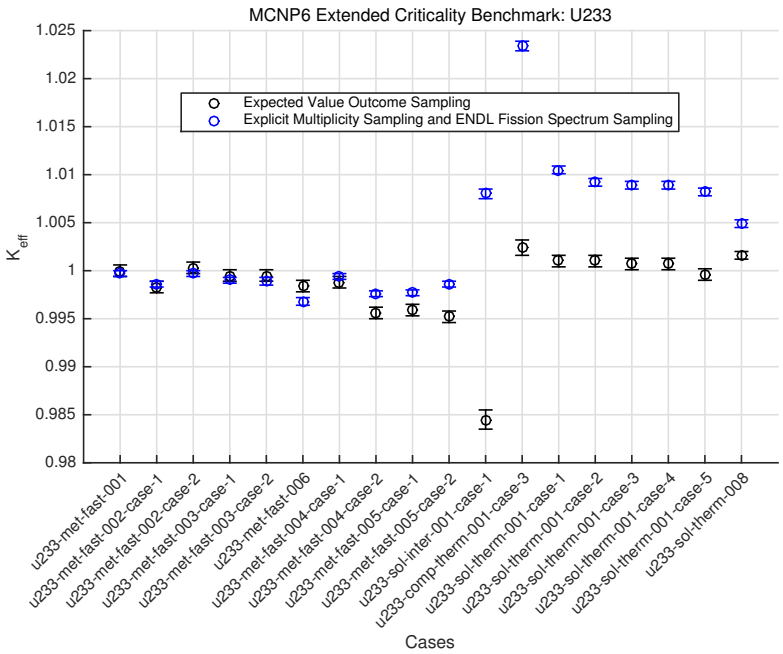

Figure 4.13: k-effective Comparisons with ENDL Fission Spectra Sampling for U233 Systems

4.6 Conclusions

Good agreement was found for expected-value outcome and explicit fission multiplicity sampling with ACE (ENDF) fission neutron spectra data. Some differences exist but are found to be at most three standard deviations from the calculated expected-value outcome k-effective. Explicit fission multiplicity sampling k-effective and $\bar{\nu}$ agrees well with default expected-value outcome sampling.

Expected-value outcome and explicit fission multiplicity sampling k-effectives using both the ENDF and ENDL neutron fission spectra showed substantial disagreements. This was expected due to the differences in models used for major actinides in the benchmarks. For cases where ENDF and ENDL fission neutron energy spectra were similar showed improved agreement. Due to differences in the ENDF and ENDL evaluations, it is recommended that ENDL prompt fission spectra data not be used in the calculation of k-effective.

Chapter 5

k_{eff} Sensitivity to $\bar{\nu}$ and $\chi(E)$ for Fission Neutron Sampling Methods

MCNP6 allows for the calculation of sensitivity coefficients of the effective multiplication k for nuclear data. Sensitivity coefficients are useful for determining which nuclear data parameters contribute most to uncertainty in k-effective values and are a simple way to determine if two systems are neutronically similar. Using MCNP6, the sensitivity coefficient for $\bar{\nu}$ was calculated for MCNP6 criticality benchmarks using linear-perturbation theory using adjoint weighting [13]. These sensitivity coefficients were used to gain insight into the effect of $\bar{\nu}$ and $\chi(E)$ uncertainty in k-effective of the various benchmarks using the two different sampling methods introduced in the previous chapters. A brief introduction into the theory of sensitivity analysis is provided in the following section. Results and analysis of sensitivity coefficients for the default MCNP6 code, multiplicty-enabled MCNP6, and multiplicity-enabled and fission neutron spectrum sampling from the LLNL Fission Library MCNP6 are discussed in the following sections.

5.1 Brief Introduction to Sensitivity Theory

A sensitivity coefficient for the multiplication factor k is the ratio of the resulting relative change in k in response to a relative change in some nuclear data parameter (Σ_f, Σ_a, ν, etc.) over a small energy range E to $E + dE$. If the change in some parameter x is small enough so that k changes linearly with respect to x, the following relationship is found:

$$S_{k,x} = \frac{\Delta k/k}{\Delta x/x} = \frac{x}{k}\frac{dk}{dx}. \tag{5.1}$$

To determine the sensitivity coefficient $S_{k,x}$ for an entire multiplying system, the k-eigenvalue neutron transport equation

$$\begin{aligned}(\hat{\Omega}\cdot\nabla + \Sigma_t)\Psi(\vec{r},\hat{\Omega},E) = &\iint dE'\; d\hat{\Omega}\;\Sigma_s(E'\to E,\hat{\Omega}'\to\hat{\Omega})\Psi(\vec{r},\hat{\Omega}',E') \\ &+ \frac{1}{k_{\text{eff}}}\iint dE'\; d\hat{\Omega}'\;\chi(E'\to E)\nu\Sigma_f(E')\Psi(\vec{r},\hat{\Omega}',E')\end{aligned} \tag{5.2}$$

is differentiated with respect to nuclear data parameter x and multiplied by x. The expression is then multiplied by the adjoint function (importance function) and the properties of the adjoint function are used to derive the following relationship for the sensitivity coefficient:

$$S_{k,x} = -\frac{\langle\psi^\dagger, (\Sigma_x - C_x - k^{-1}F_x)\psi\rangle}{\langle\psi^\dagger, F\psi\rangle}. \tag{5.3}$$

where ψ is the neutron angular flux and $\psi^{\dagger}$ is the adjoint angular flux, Σ_x is the cross section for the nuclear data parameter x and is zero if x is not a cross section. C_x is the integral scattering operator and $k^{-1}F_x$ is the integral fission operator for x. These operators are zero for the case where x is not a scattering operator only for x or a fission operator only for x respectively. F is the integral fission operator for the entire system.

The fission spectra χ has the constraint that its integral normalize to one. To satisfy this requirement, the sensitivity coefficient is modified to

$$\hat{S}_{k,f}(E', E) = S_{k,f}(E', E) - f(E' \rightarrow E) \iint dE \; S_{k,f}(E', E). \tag{5.4}$$

The magnitude of a sensitivity coefficient is proportional to the impact on a system's k-effective of that a small change in the nuclear data parameter creates. The sign of the sensitivity coefficient determines the direction of the change in the multiplication factor for a corresponding change in x. Sensitivity coefficients are also additive. The sensitivity coefficient of the total energy integrated average number of neutrons emitted per fission $\bar{\nu}$ is equal to the sum of the sensitivity coefficients of $\bar{\nu}$ over some energy partitioning. Likewise, for the fission neutron energy spectrum, the overall sensitivity coefficient for χ is the sum of sensitivity coefficients over a partitioning of the incoming and emitted neutron energy ranges.

5.2 k-effective Sensitivity of MCNP6 Criticality Benchmarks to $\bar{\nu}$

Five systems in Table 5.1 were selected from the MCNP6 Criticality Validation Suite for comparison. These five benchmarks were selected based on the level of agreement or disagreement for k-effectives between the expected-value outcome approach and explicit fission multiplicity sampling. The cases selected were: FLAT23, GODIVA, ORNL11, PNL33, and JEZPU. The input files for each case can be seen in Appendix A.

Cases	k-effective (Explicit Fission Multiplicity)	Uncertainty	k-effective (Expected-Value Outcome Sampling)	Uncertainty	Δk	Uncertainty
FLAT23	0.999	0.0003	0.9983	0.0002	0.0007	0.0004
GODIVA	0.9998	0.0002	1.0000	0.0002	-0.0002	0.0003
ORNL11	1.0015	0.0003	1.0015	0.0001	0.0000	0.0003
PNL33	1.007	0.0003	1.0063	0.0002	0.0007	0.0004
JEZPU	0.9993	0.0002	0.9996	0.0002	-0.0003	0.0003

Table 5.1: MCNP6 Expected-Value Outcome, Explicit Multiplicity Sampling Sensitivity Study Cases

5.2.1 k-effective Sensitivity of FLAT23 to $\bar{\nu}$

The FLAT23 system was found to have one of the largest differences in k-effectives (0.0007 ± 0.004) for the sampling methods. The sensitivity plot seen in Figure 5.1 over 0.01 MeV to 20 MeV for uranium-233 shows little difference in the system's sensitivity to $\bar{\nu}$. The explicit fission multiplicity and expected-value outcome sampling methods showed good agreement despite overall disagreement in k-effective. This strongly suggested differences in the neutron fission spectra for both sampling methods.

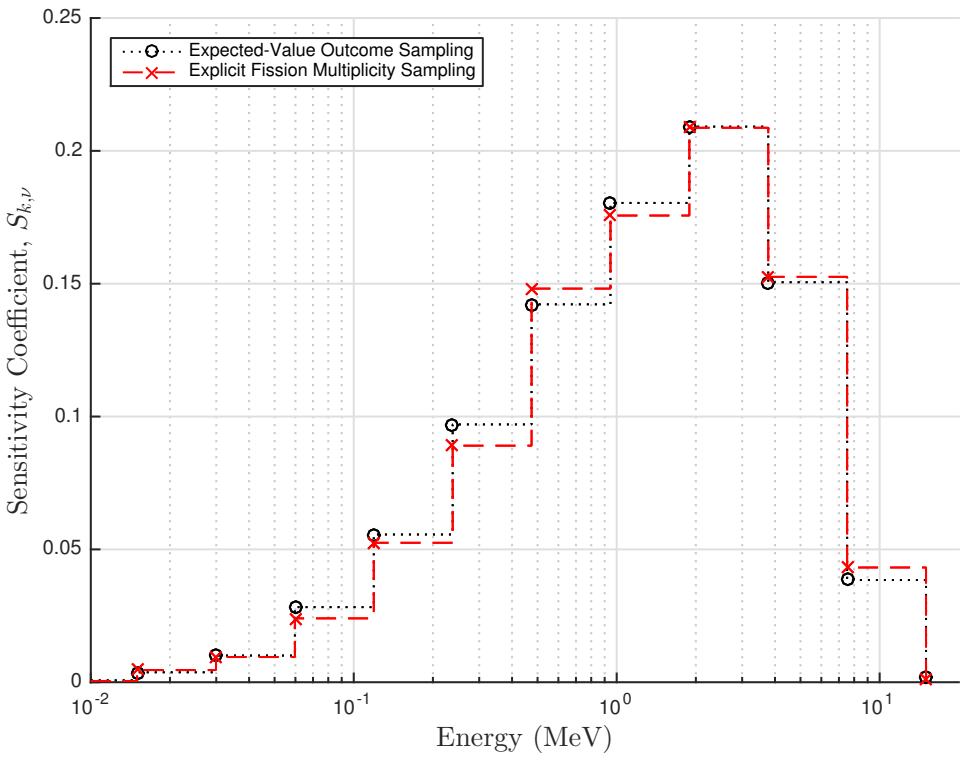

Figure 5.1: k-effective Sensitivity of FLAT23 to Uranium-233 $\bar{\nu}$

5.2.2 k-effective Sensitivity of GODIVA to $\bar{\nu}$

The GODIVA system showed a small k-effective difference of -0.0002 for both sampling methods. The sensitivity plot to uranium-235 $\bar{\nu}$ in Figure 5.2 demonstrates similar sensitivity profiles over the energy range of 0.01 MeV to 20 MeV. Differences exist in the intermediate portion of the profile, accounting for the differences in k-effective. These differences are small, and the systems are shown to be neutronically similar.

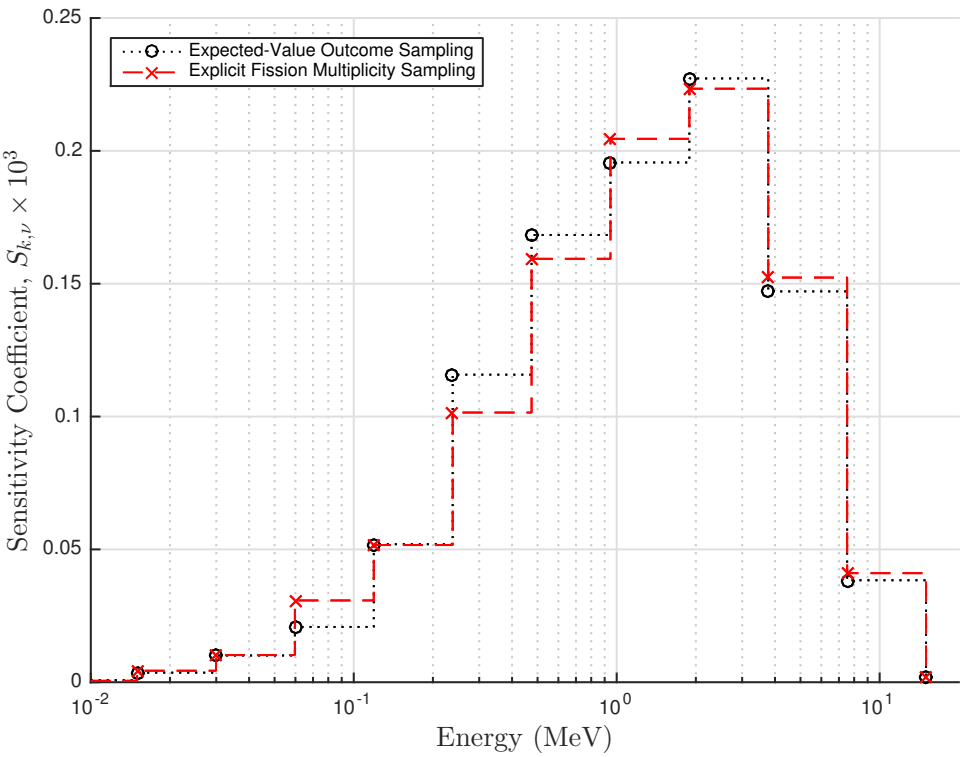

Figure 5.2: k-effective Sensitivity of GODIVA to Uranium-235 $\bar{\nu}$

5.2.3 k-effective Sensitivity of ORNL11 to $\bar{\nu}$

The ONRL11 case has uranium-233 as its primary fissile constituent. The ORNL11 system showed minimal differences between both the expected-value outcome and explicit fission sampling methods. The sensitivity profiles in Figure 5.3 of the system to uranium-233 $\bar{\nu}$ showed good agreement with sensitivity coefficients on the order of 1×10^{-4}.

^{233}U Average Number of Neutrons Emitted in Fission $\bar{\nu}$ Sensitivity-ORNL11

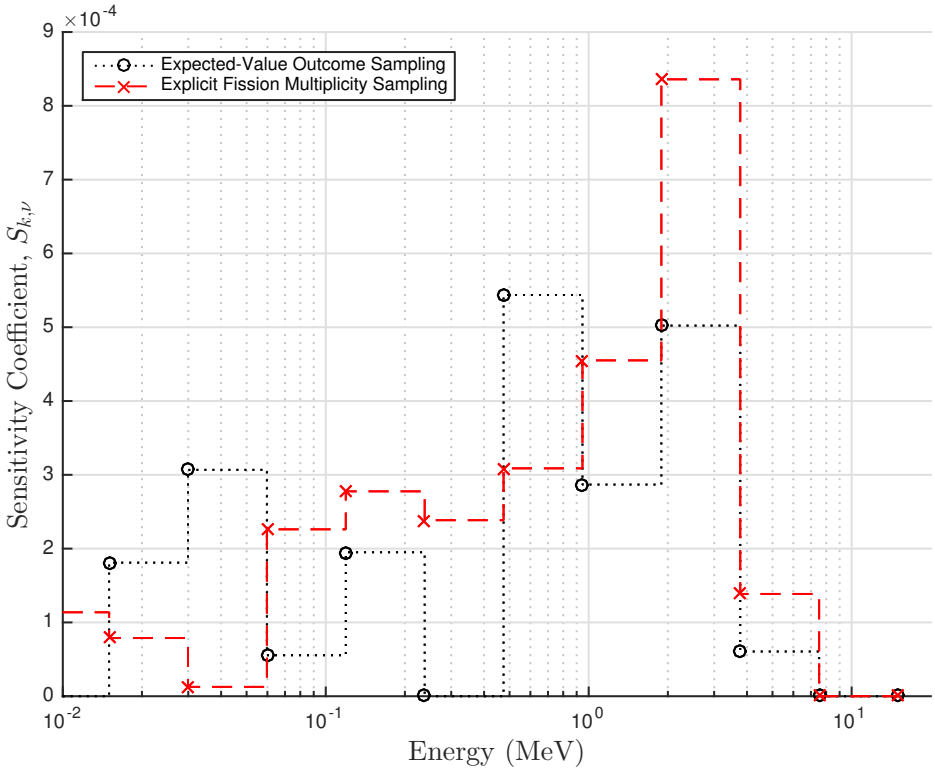

Figure 5.3: k-effective Sensitivity of ORNL11 to Uranium-233 $\bar{\nu}$

5.2.4 k-effective Sensitivity of PNL33 to $\bar{\nu}$

The PNL33 system k-effectives showed disagreement between the two sampling methods of 0.0007. The sampling profile seen in Figure 5.4 showed small differences in the sensitivity profile for plutonium-233 throughout the energy domain. The similar sensitivity coefficients suggest differences in k-effective were driven by different in the prompt neutron fission spectrum though this was not found to be a case. These systems are neutronically similar and differences in k-effective are due to other factors.

^{239}Pu Average Number of Neutrons Emitted in Fission $\bar{\nu}$ Sensitivity-PNL33

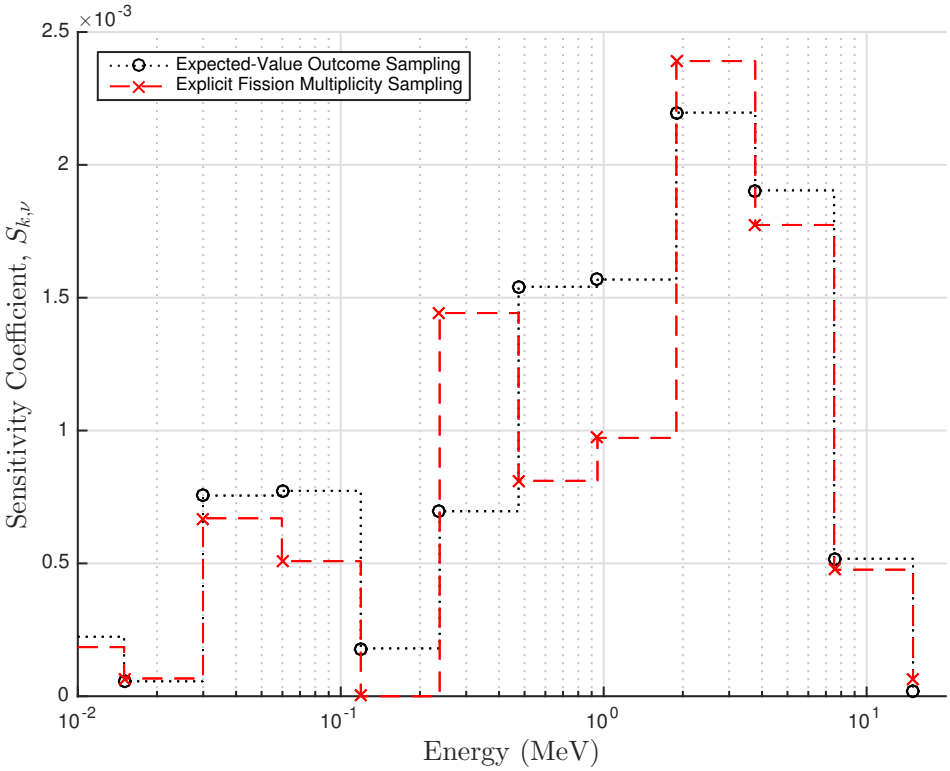

Figure 5.4: k-effective Sensitivity of PNL33 to Plutonium-239 $\bar{\nu}$

5.2.5 k-effective Sensitivity of JEZPU to $\bar{\nu}$

The JEZPU system showed k-effective disagreement of -0.0003 and the sensitivity profile in Figure 5.5 showed similar neutronic sensitivity profiles to $\bar{\nu}$. Differences in the k-effective values despite similar $\bar{\nu}$ sensitivity profiles suggest differences in sensitivity profiles of the fission neutron emission spectrum which can be seen in the next section.

^{239}Pu Average Number of Neutrons Emitted in Fission $\bar{\nu}$ Sensitivity-JEZPU

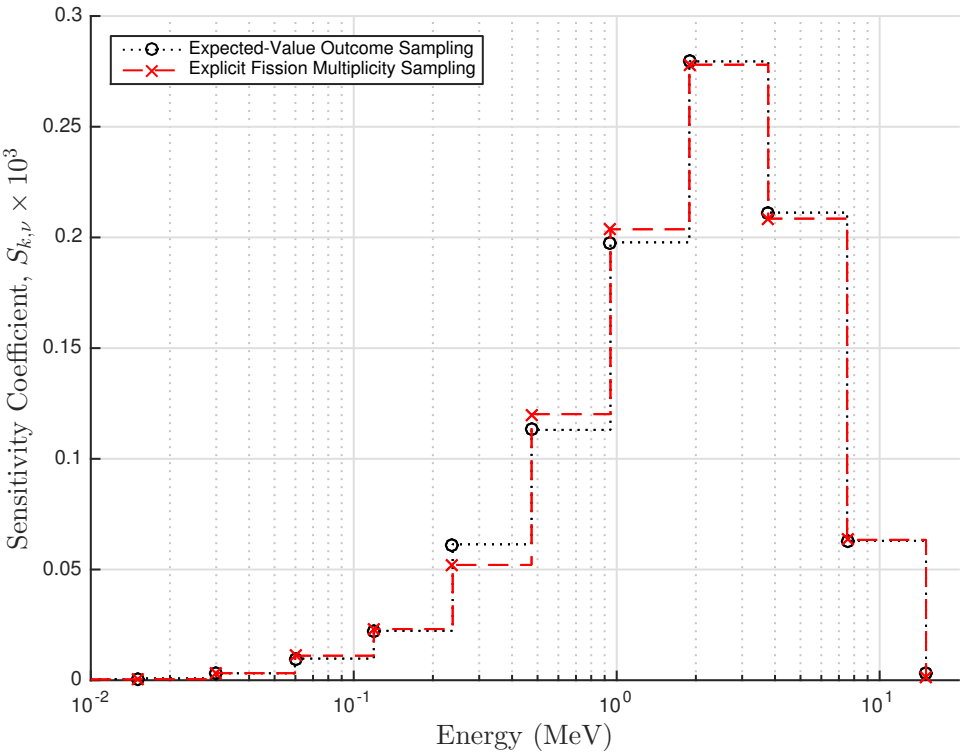

Figure 5.5: k-effective Sensitivity of JEZPU to Plutonium-239 $\bar{\nu}$

5.3 k-effective Sensitivity of MCNP6 Criticality Benchmarks to $\chi(E)$

The same five systems were selected from the MCNP6 Criticality Validation Suite for fission neutron emission spectrum comparisons. Sensitivity to neutron fission energy spectra determines the average energy of the neutron entering the system after fission that has an impact on k-effective through $\bar{\nu}$ in both the expected-value outcome sampling and explicit fission multiplicity sampling methods. Differences in k-effective can be attributed to differences in both $\bar{\nu}$ and $\chi(E)$ and are examined to determine similarity between benchmark cases.

5.3.1 k-effective Sensitivity of FLAT23 to $\chi(E)$

The FLAT23 system shows slight sensitivity differences in the upper energy bins as seen in Figure 5.6. In particular, explicit fission multiplicity shows greater sensitivity relative to expected-value outcome sampling in the upper energy bins.

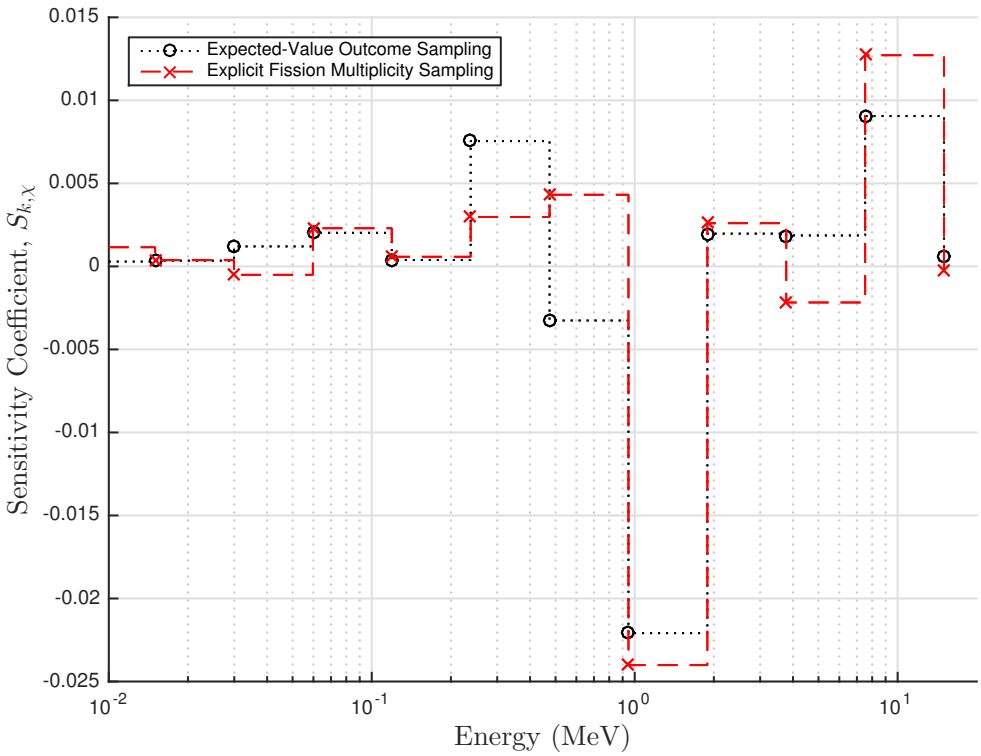

Figure 5.6: k-effective Sensitivity of FLAT23 to Uranium-233 $\chi(E)$

5.3.2 k-effective Sensitivity of GODIVA to $\chi(E)$

There are small differences in the fission neutron energy spectrum sensitivity profiles. Differences exist in some upper energy bins as seen in Figure 5.7 but overall agreement

is good as the differences in k-effective between the two sampling methods was -0.0002.

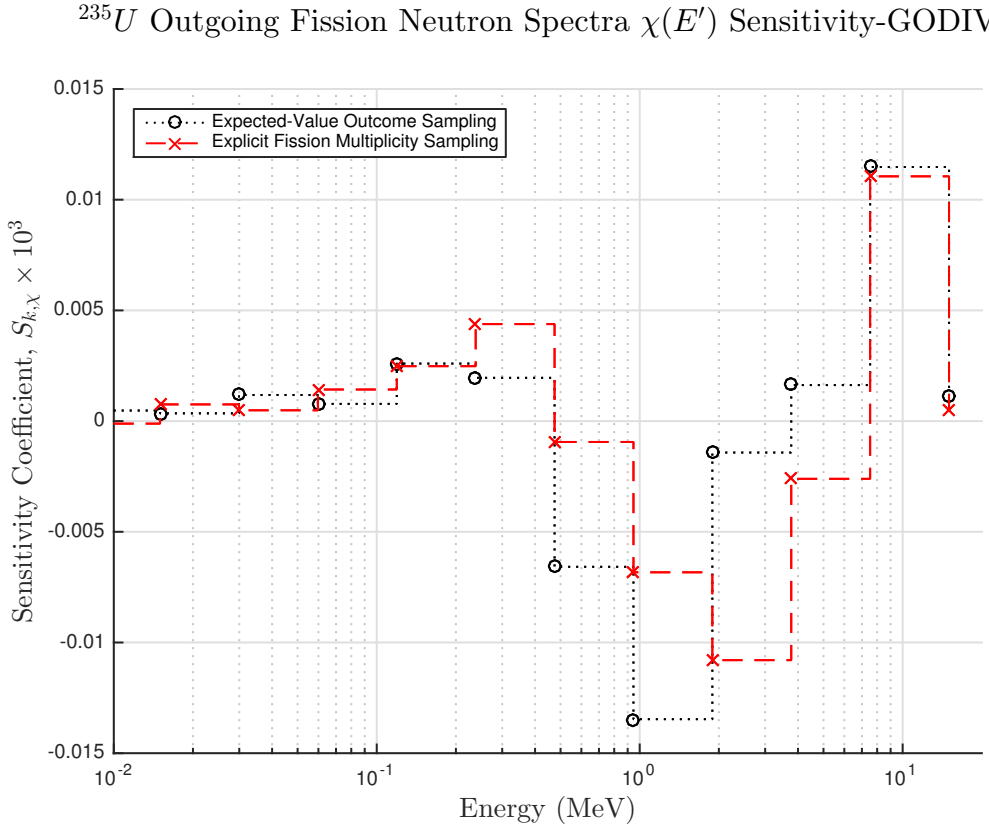

Figure 5.7: k-effective Sensitivity of GODIVA to Uranium-235 $\chi(E)$

5.3.3 k-effective Sensitivity of ORNL11 to $\chi(E)$

Differences in the neutron fission energy spectrum sensitivities were apparent especially at higher energy bins. Despite this, k-effectives were in perfect agreement and sensitivity coefficients only differ by a magnitude of 1×10^{-2}. This reflects two neutronically similar systems as shown in Figure 5.8.

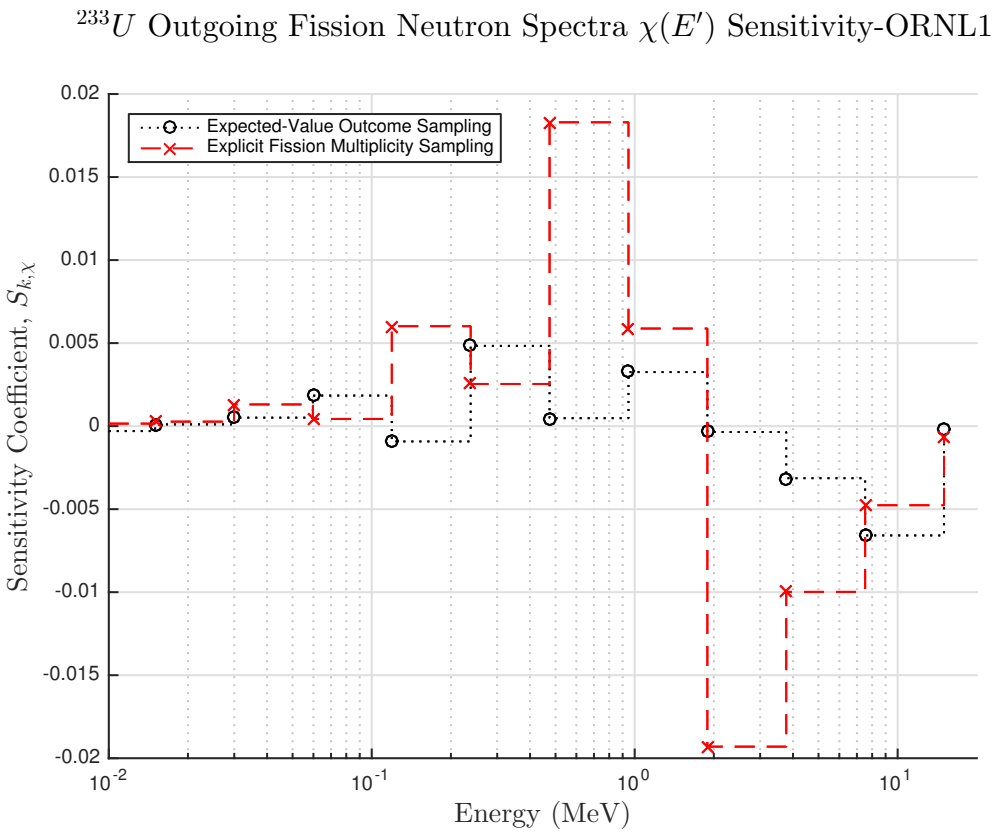

Figure 5.8: k-effective Sensitivity of ORNL11 to Uranium-233 $\chi(E)$

5.3.4 k-effective Sensitivity of PNL33 to $\chi(E)$

Differences in the neutron fission energy spectrum sensitivities at higher energy bins reflect neutronically dissimilar systems. Sensitivity coefficients for expected-value outcome and explicit fission multiplicity sampling alternate in importance in the upper energy range reflecting neutronically dissimilar systems as seen in Figure 5.9 though the overall magnitude of sensitivity coefficients are on the order of 1×10^{-3}.

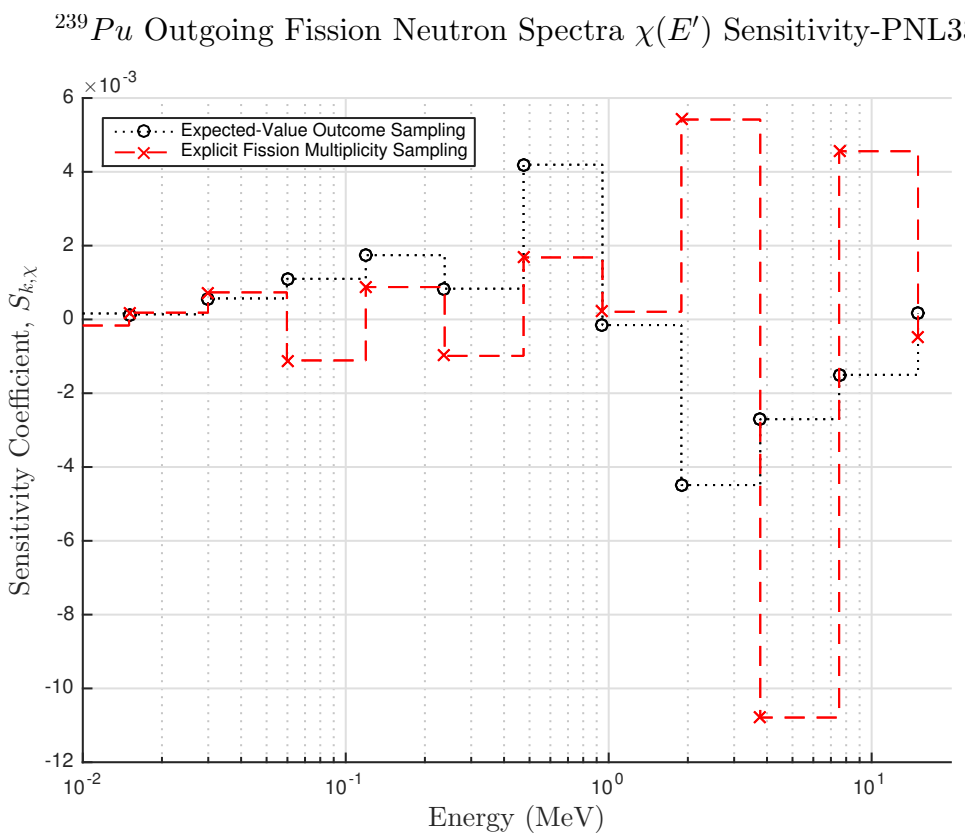

Figure 5.9: k-effective Sensitivity of PNL33 to Plutonium-239 $\chi(E)$

5.3.5 k-effective Sensitivity of JEZPU to $\chi(E)$

k-effective differences in sampling methods for the JEZPU system can be seen in the dissimilar sensitivity profiles for $\chi(E)$. As seen in Figure 5.10, the systems are most dissimilar at higher energy bins and for a fast system such as JEZPU causes differences in k-effective values for the sampling methods.

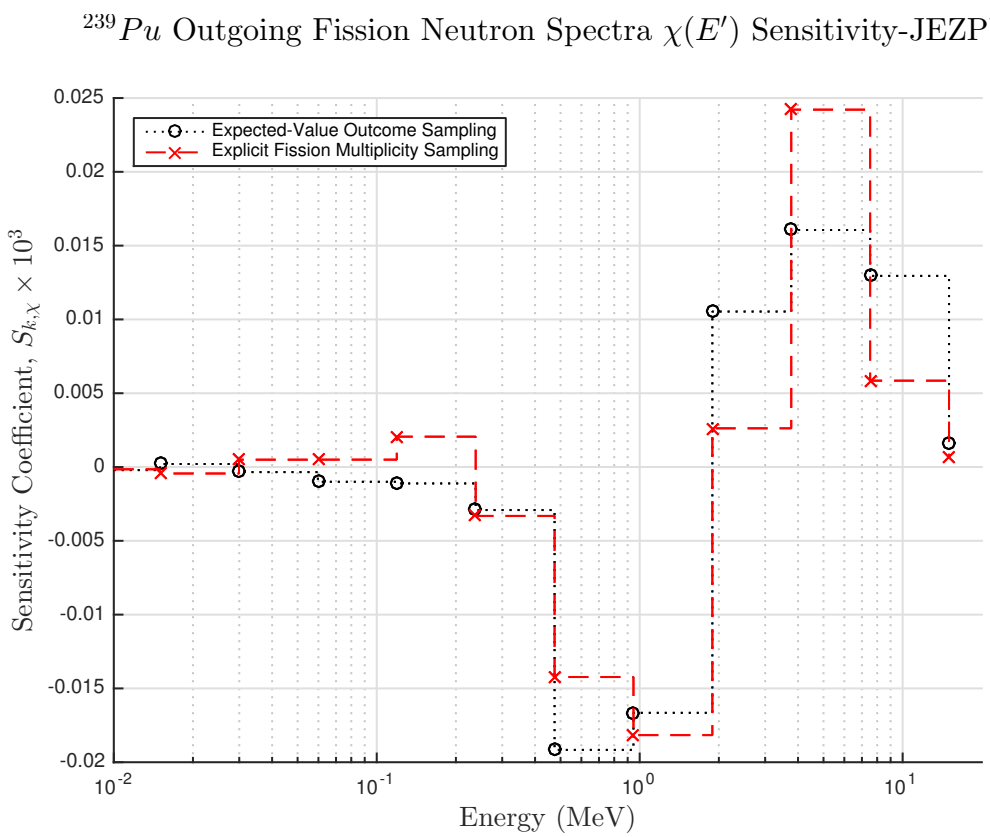

Figure 5.10: k-effective Sensitivity of JEZPU to $\chi(E)$

5.4 Conclusion

Sensitivity coefficients allow for a measure of neutronic similarity between two systems for particular nuclear data parameters. Their use in the testing of the explicit fission multiplicity sampling implementation in MCNP6 allows insight into the changes to k-effective as a function of the nuclear data terms driving k-effective calculations. Clear trends emerge that reflect the calculated changes in k-effective for the two sampling methods. Systems found in agreement using both schemes show similar sensitivity profiles while systems showing greater k-effective differences show dissimilar sensitivity profiles.

Chapter 6

Uncertainty Propagation of $\bar{\nu}$ in k-effective Calculations

The increased reliance on computational methods for the calculation of k-effective values for nuclear systems has made it necessary to determine the uncertainties in results due to computational methods and nuclear data [4]. In particular, nuclear data uncertainties continue to remain one of the largest sources of uncertainty in calculations. It is necessary to establish uncertainty in calculated k-effective values for all sorts of systems. In this chapter, two methods of nuclear data uncertainty propagation are explored: the Total Monte Carlo Method and Sensitivity Analysis using sensitivity coefficients. For the Total Monte Carlo Method ENDF/B-VII.1 covariance data for the major actinides (U-235, U-238, and Pu-239) were used to generate realizations of $\bar{\nu}$ in MCNP6 ACE (A Compact ENDF) files and then were ran using MCNP6 to calculate k-effective. For the calculation of uncertainty using sensitivity coefficients, the MCNP6 KSEN method was used. An explanation of both methods follows with the comparison of uncertainty from both methods using various benchmark cases from the MCNP6 Criticality Benchmark.

6.1 $\bar{\nu}$ Covariances in ENDF/B-VII.1

A cross section or related quantity such as $\bar{\nu}$ in an ENDF file represents a physical quantity that has a definite though unknown magnitude. How well known a value is known is represented by its density function, defined such that $f(\bar{\nu})\ \Delta\bar{\nu}$ is the probability that the true value of $\bar{\nu}$ lies in the range $\Delta\bar{\nu}$ about $\bar{\nu}$. The marginal density function $f(\bar{\nu})$ is the average over all other independent variables of the overall density function of the cross section data. The density function is normalized to one for all variables.

Quantities in an ENDF file are expected values for nuclear data parameters. The expected value of a function, $\langle f(\bar{\nu})\rangle$, is the average value of that function over its density function. The expected value of a function is given by

$$\langle\bar{\nu}\rangle = \int \bar{\nu}\ f(\bar{\nu})\ d\bar{\nu}. \tag{6.1}$$

The true value of an quantity such as $\bar{\nu}$ is then defined to be $\bar{\nu} = \langle\bar{\nu}\rangle + \delta\bar{\nu}$ where $\langle\delta\bar{\nu}\rangle = 0$.

ENDF/B-VII.1 file formats contain only expected values of nuclear data quantities and the second degree-moments of the joint density function describing the true value of a nuclear data vector [10]. Second moments of the density function are related using the covariance. If $\langle\bar{\nu}(E_i)\rangle$ and $\langle\bar{\nu}(E_j)\rangle$ are the expected value of the number of neutrons emitted in fission at energies E_i and E_j and $f(\bar{\nu}(E_i), \bar{\nu}(E_j))$ is the joint density function for $\bar{\nu}(E_i)$ and $\bar{\nu}(E_j)$, the covariance between the two values is defined as:

$$\begin{aligned}\mathrm{Cov}(\bar{\nu}(E_i), \bar{\nu}(E_j)) &= \langle \delta\bar{\nu}(E_i)\ \delta\bar{\nu}(E_j)\rangle \\ &= \iint (\bar{\nu}(E_i) - \langle\bar{\nu}(E_i)\rangle)\ (\bar{\nu}(E_j) - \langle\bar{\nu}(E_j)\rangle)\ f(\bar{\nu}(E_i)\ \bar{\nu}(E_j))\ d\bar{\nu}(E_i)\ d\bar{\nu}(E_j).\end{aligned} \tag{6.2}$$

The variance of $\bar{\nu}(E_i)$ is defined as:

$$\mathrm{Var}(\bar{\nu}(E_i)) = \mathrm{Cov}(\bar{\nu}(E_i), \bar{\nu}(E_i)) = \langle \delta\bar{\nu}(E_i)^2\rangle, \tag{6.3}$$

and the uncertainty as

$$\sigma(\bar{\nu}(E_i)) = [\mathrm{Var}(\bar{\nu}(E_i)]^{1/2}. \tag{6.4}$$

For some major actinides, covariance values for $\bar{\nu}$ are given in terms of the relative covariance:

$$\mathrm{Rcov}(\bar{\nu}(E_i), \bar{\nu}(E_j)) = \mathrm{Cov}(\bar{\nu}(E_i), \bar{\nu}(E_i))/[\sigma(\bar{\nu}(E_i))\ \sigma(\bar{\nu}(E_j))]. \tag{6.5}$$

Knowledge of covariance data for major actinides allows for the calculation of uncertainty of calculated k-effectives.

$\bar{\nu}$ covariances for major actinides are given in ENDF files for a single list of energies E_k that specify the energy intervals over which the covariance matrix is analyzed [10]. Major actinide covariances are listed in File 33 of the ENDF/B-

VII.1 data files and are given an FLAG LB=5. FLAG LB=5 listed covariances are fractional covariance values and the actual covariance value must be calculated from the expression

$$\mathrm{Cov}(X_i, Y_j) = \sum_{k,k'} \mathcal{P}^{i;k}_{j,k'} F_{xy;k,k'} X_i Y_j \tag{6.6}$$

where

$$\mathcal{P}^{i;k}_{j,k'} \equiv \mathcal{S}^k_i \mathcal{S}^l_i ... \mathcal{S}^m_j \mathcal{S}^n_j ..., \tag{6.7}$$

where

$\mathcal{S}^k_i \equiv 1$ when $E_k \leq E_i \leq E_{k+1}$ and $\mathcal{S}^k_i \equiv 0$ when the energy E_i is outside the range of E_k to E_{k+1}. $F_{xy;k;k'}$, X_i, and Y_j are the fractional covariance, and expected values at energies E_i and E_j respectively. The covariance matrices for the average number of neutrons emitted per fission for the major actinides were generated using ENDF/B-VII.1 data.

From the average number of neutrons emitted per fission covariance matrices, correlation matrices for the major actinides are calculated. A correlation matrix consists of correlation coefficients that describe how to values are related. Correlation coefficients are measured between -1 (implies anti-correlation) and 1 (perfectly correlated). Correlation coefficients are calculated using the following expression

$$\rho_{X_i,Y_j} = \mathrm{Corr}(X_i, Y_j) = \frac{\mathrm{Cov}(X_i, Y_j)}{\sigma_{X_i} \sigma_{Y_j}}. \tag{6.8}$$

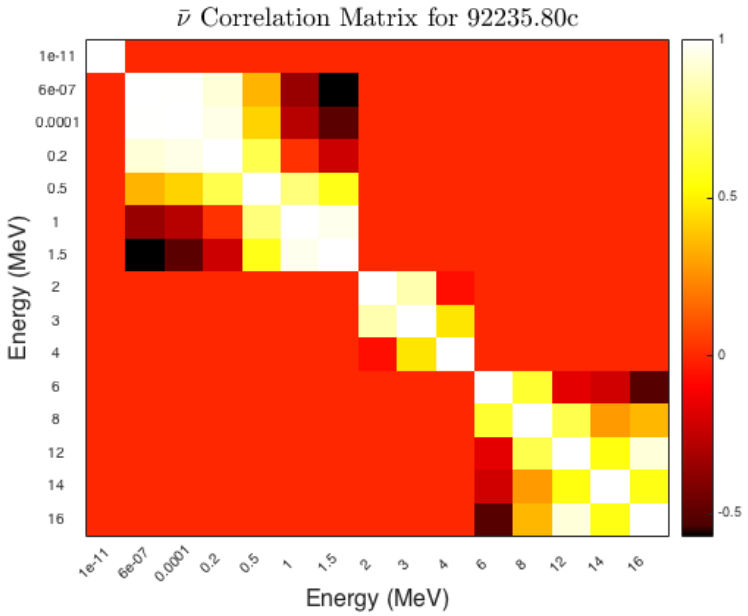

Figure 6.1: Average Number of Neutrons Emitted in Fission Correlation Matrix for Uranium-235

Correlation matrices for uranium-235, uranium-238, and plutonium-239 can be seen in Figures 6.1, 6.2, and 6.3 respectively.

One current limitation to using ENDF/B-VII.1 covariance data is the lack of detailed covariance parameters for quantities of interest. For example, the major actinides uranium-235 and uranium-238 only have a few energy groups over which covariance parameters have been analyzed, fifteen and five energy groups respectively. This is in stark contrast to the other major actinide, plutonium-239, whicj has covariance data for 50 energy groups.

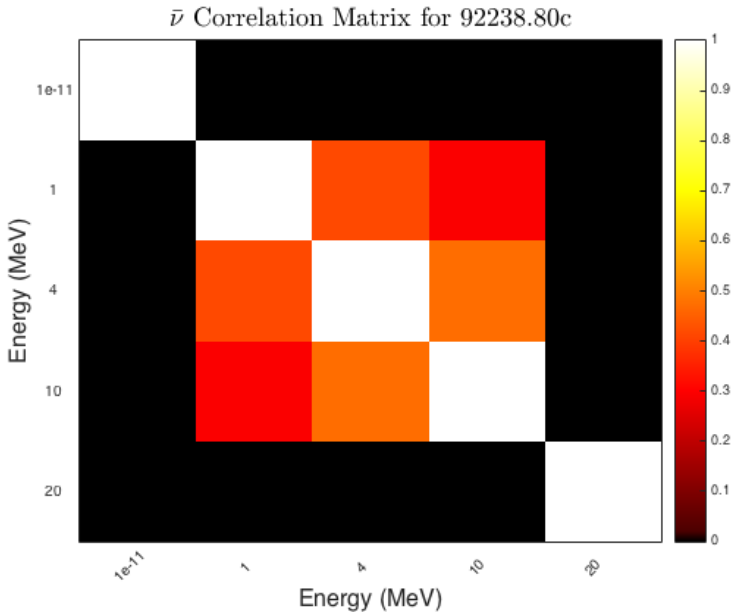

Figure 6.2: Average Number of Neutrons Emitted in Fission Correlation Matrix for Uranium-238

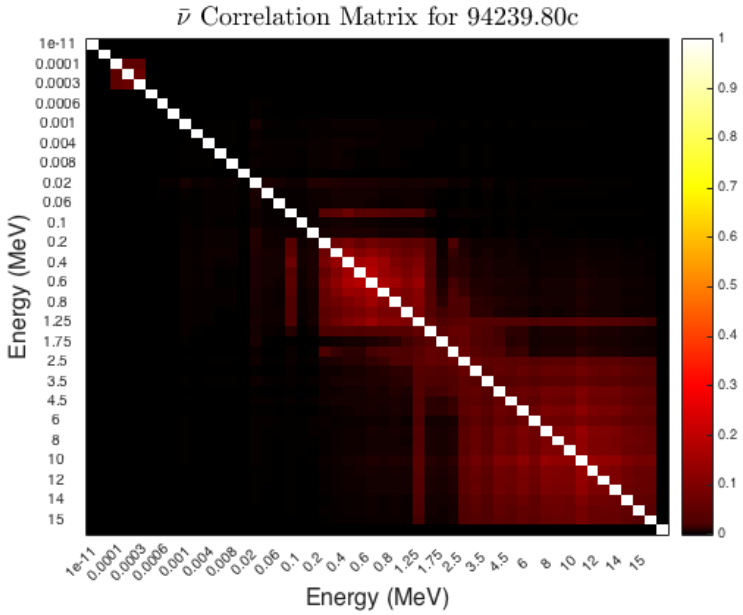

Figure 6.3: Average Number of Neutrons Emitted in Fission Correlation Matrix for Plutonium-239

6.2 The Total Monte Carlo Method

The Total Monte Carlo Method [18] uses ENDF/B-VII.1 covariance data to generate random realizations of $\bar{\nu}$ for major actinides. These files are then used in MCNP6 calculations to calculate k-effective and generate a probability distribution function for k-effective where an normal distribution is then fitted to determine uncertainty in k-effective.

Given a $\bar{\nu}$ covariance matrix Σ over some energy interval divided into N segments $E_i \leq E \leq E_N$, a vector of correlated $\bar{\nu}$ values can be generated through the following process: it is necessary to find a matrix L such that

$$L^T L = \Sigma \tag{6.9}$$

where L is an upper or lower triangular matrix. L is usually obtained through a Cholesky decomposition or an eigenvector decomposition of the covariance matrix Σ and various software packages allow for its quick evaluation. Given L, a vector of random, normally distributed numbers $\vec{R}$ can be multiplied by L as follows to obtain a vector R_C of correlated, random values:

$$\vec{R}_C = \vec{R}L. \tag{6.10}$$

The vector of normally-distributed, correlated values $\vec{R}_C$ is then added to the expected value of average number of neutrons emitted per fission $\bar{\nu}$ at that energy interval to generate a random, correlated vector of $\bar{\nu}$ values.

$$\vec{\bar{\nu}}_C = \vec{\bar{\nu}} + \vec{R}_C. \tag{6.11}$$

Three user written MATLAB scripts, one each for uranium-235, uranium-238, and plutonium-239 (see Appendix B) were used to generate one thousand realizations of normally-distributed, correlated $\bar{\nu}$ values and their nuclear data cross section files for use in MCNP6. One challenge to this methodology is the structure of covariance data in ENDF data files [17]. Since ENDF/B-VII.1 $\bar{\nu}$ covariance data for the major actinides does not cover the entire energy range over which $\bar{\nu}$ are listed, it was necessary to interpolate the normal-distributed, correlated values over the entire energy grid. Using the ENDF listed interpolation scheme, data files containing the new total average number of neutrons emitted in fission were created.

ACE (A Compact ENDF) files were generated using a MATLAB script. MCNP6 benchmark files containing major actinides were modifed to allow for the use of the generated ACE files. The MCNP6 card `XSn` was used to allow MCNP6 to access and sample from the newly generated files. A bash script was used to loop over the different ACE file realizations and k-effective, standard deviation, and the average number of neutrons emitted in fission were recorded. k-effective values were used to generate a probability distribution function of k-effective. The MATLAB routine `fitdist` was used to fit a normal distribution to the probability distribution function with the same mean and uncertainty in k-effective as a result of nuclear data and statistical uncertainties. To determine the uncertainty due to nuclear data, it is necessary to remove the uncertainty from statistics. If σ^2_{obs} is the observed variance of the probability distribution function, the observed variance can be calculated as the sum of the variances due to nuclear data σ^2_{ND} and statistics σ^2_{stat}:

$$\sigma_{obs}^2 = \sigma_{ND}^2 + \sigma_{\text{stat}}^2. \tag{6.12}$$

To eliminate the statistical uncertainty, the following argument from [1] is used: because MCNP6 returns both k-effective and the standard deviation in k-effective, the mean of the standard deviations $\Delta\bar{k}_{\text{eff}}$ for the N different ACE file realizations is equal to σ_{stat} assuming there is no correlation between statistics and nuclear data. Subtracting the variance due to statistics, the uncertainty in k_{eff} due to uncertainty in nuclear data, in this case $\bar{\nu}$, can be determined using the Total Monte Carlo approach.

6.3 Sensitivity Analysis

An alternative method for the calculation of the uncertainty due to nuclear data is through the use of sensitivity coefficients. Sensitivity coefficients are used to propagate uncertainty to the calculated k-effective value. Given uncertainty information for a nuclear data parameter such as $\bar{\nu}$, it is possible to estimate the uncertainty in the system multiplication factor due to the uncertainties in the data. The following explanation is from [4]: given a nuclear data parameter (α_n), α is an M length vector where M is the number of nuclear data parameter reaction pairs (cross sections, average number of neutrons emitted in fission, fission neutron spectrum, etc.) $\times$ the number of energy groups being analyzed. There is a corresponding M $\times$ M matrix containing the relative variances and covariances in the nuclear data and it is defined as

$$\mathbf{C}_{\alpha\alpha} \equiv \left[\frac{\mathrm{cov}(\alpha_n, \alpha_p)}{\alpha_n \alpha_p}\right] \tag{6.13}$$

$$n, p = 1, 2, ..., M$$

where

$$\mathrm{Cov}(\alpha_n, \alpha_p) = \langle \delta\alpha_n \delta\alpha_p \rangle \tag{6.14}$$

where the covariances are integrated over the ranges of α_n and α_p weighted with some probability distribution function.

We are only interested in $\bar{\nu}$ and in the cases where only one nuclear data parameter is being considered, the covariance matrix $\mathbf{C}_{\alpha\alpha}$ reduces to the relative covariance matrix for $\bar{\nu}$ found in ENDF/B-VII.1 data files.

Sensitivities of k-effective to nuclear data parameters α_n are contained in a matrix $\mathbf{S_k}$ defined as:

$$\mathbf{S_k} \equiv \left[\frac{\alpha_n}{k_i}\frac{\partial k_i}{\partial \alpha_n}\right], \quad i = 1, 2, ..., I \tag{6.15}$$

where I is the number of critical systems considered and n is defined as before. For the case where only one critical system is considered, $\mathbf{S_k}$ reduces to a vector of sensitivities over M energy groups. The uncertainty matrix for a system's k-effective

can be calculated as

$$\mathbf{C_{kk}} = \mathbf{S_k} \mathbf{C}_{\alpha\alpha} \mathbf{S_k^\dagger} \tag{6.16}$$

where $\mathbf{S_k^\dagger}$ is the transpose of $\mathbf{S_k}$.

6.4 Total Monte Carlo/Sensitivity Analysis Uncertainty Comparison for $\bar{\nu}$

Calculated uncertainties in $\bar{\nu}$ using the Total Monte Carlo and Sensitivity Analysis were compared for various benchmark cases in the MCNP6 Criticality Validation Suite and some simple geometry and material cases. Uncertainties were found to agree within 10% for most cases.

6.4.1 $\bar{\nu}$ Impacts on GODIVA

GODIVA is a solid bare sphere of highly enriched uranium-235 with a fast neutron spectrum. The impact of the uncertainty on the average total number of neutrons emitted in fission was found to be 114.2 pcm using the Total Monte Carlo approach. The Total Monte Carlo k-effective distribution shows that $\bar{\nu}$ contributes very little uncertainty to the integral quantity k-effective. Figure 6.4 shows the spread of calculated k-effective values. The calculated Sensitivity Analysis uncertainty was found to be 110.0 pcm, within 4% of the TMC value. Table 6.1 shows the calculated uncertainties and ratio of reactivities.

Table 6.1: Calculated $\bar{\nu}$ Uncertainties in GODIVA

Calculated $\bar{\nu}$ Uncertainties for GODIVA					
TMC	114.2 pcm	Sens. Analysis	110.0 pcm	Ratio	1.0379

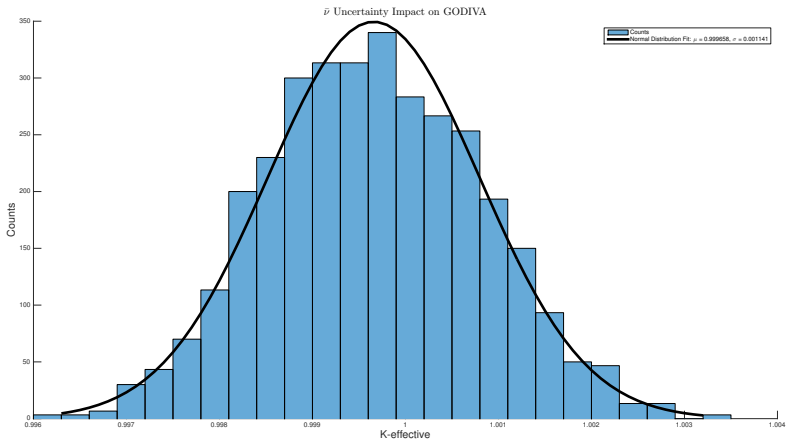

Figure 6.4: $\bar{\nu}$ Uncertainty on GODIVA

6.4.2 $\bar{\nu}$ Impacts on JEZPU

JEZPU is a solid bare metal sphere of plutonium with a fast spectrum. The total average number of neutrons emitted per fission was varied using ENDF covariance data for the fissle plutonium isotopes present in the system. The impact of the uncertainty (Figure 6.5) on the average total number of neutrons emitted in fission was found to be 107.21 pcm. Table 6.2 shows the calculated Sensitivity Analysis uncertainty of 98.13 pcm. Uncertainties were within 10%.

Table 6.2: Calculated $\bar{\nu}$ Uncertainties in JEZPU

Calculated $\bar{\nu}$ Uncertainties for JEZPU					
TMC	107.21 pcm	Sens. Analysis	98.13 pcm	Ratio	1.0925

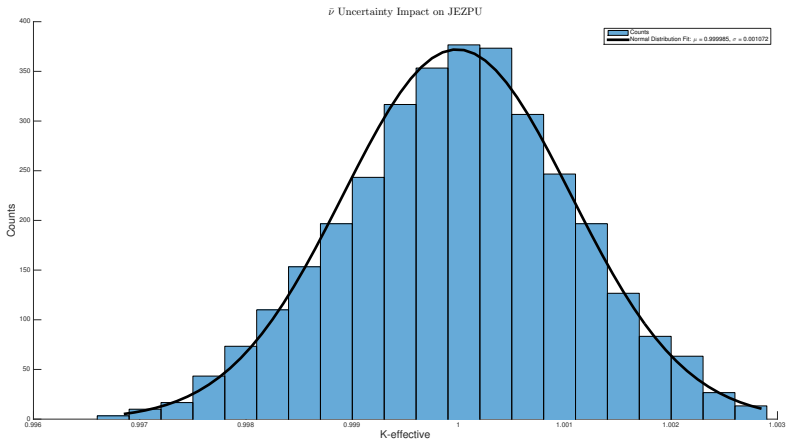

Figure 6.5: $\bar{\nu}$ Uncertainty on JEZPU

6.4.3 $\bar{\nu}$ Impacts on JEZ240

JEZPU240 is a solid bare metal sphere of plutonium primarily fueled with plutonium-239. Figure 6.6 shows the impact of $\bar{\nu}$ of k-effective. The uncertainty is k-effective was calculated as 91.75 pcm. Table 6.3 shows the calculated Sensitivity Analysis uncertainty as 89.62 pcm. Calculated uncertainties were found to be within 3%.

Table 6.3: Calculated $\bar{\nu}$ Uncertainties in JEZ240

Calculated $\bar{\nu}$ Uncertainties for JEZ240					
TMC	91.75 pcm	Sens. Analysis	89.62 pcm	Ratio	1.0238

6.4.4 $\bar{\nu}$ Impacts on FLAT25

FLAT25 is a highly enriched uranium sphere reflected by natural uranium. Figure 6.7 demonstrated the effects of $\bar{\nu}$ uncertainty on the system k-effective. The k-effective uncertainty was determined to be 109.36 pcm as compared to 99.57 pcm for Sensitivity Analysis as seen in Table 6.4.

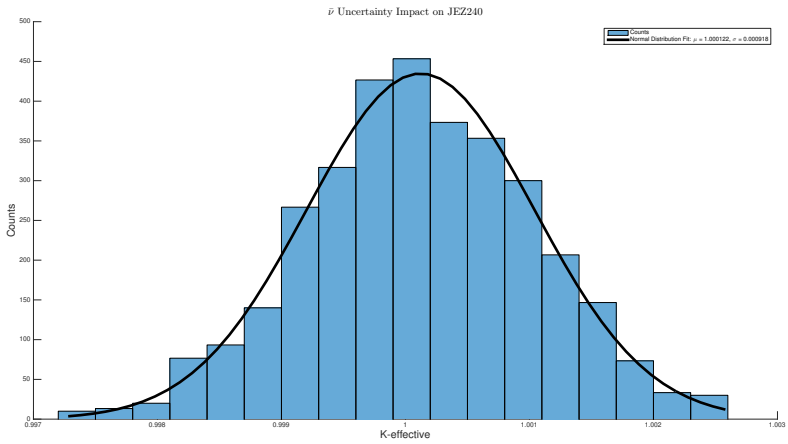

Figure 6.6: $\bar{\nu}$ Uncertainty on JEZ240

Table 6.4: Calculated $\bar{\nu}$ Uncertainties in FLAT25

Calculated $\bar{\nu}$ Uncertainties for FLAT25					
TMC	109.36	Sens. Analysis	99.57 pcm	Ratio	1.0983

6.4.5 $\bar{\nu}$ Impacts on JezPu239

JezPu239 is a sphere of plutonium-239 used to determine the uncertainty of the total average number of neutrons emitted in fission of the ENDF evaluation of plutonium-239 nuclear and covariance data. The simple system was unreflected and used to demonstrate the method for determining uncertainty in other criticality benchmark cases. The calculated uncertainty in $\bar{\nu}$ was found to be 10 pcm. For Sensitivity Analysis, the calculated uncertainty was found to be 10.36 pcm as seen in Table 6.5.

Table 6.5: Calculated $\bar{\nu}$ Uncertainties in JezPu239

Calculated $\bar{\nu}$ Uncertainties for JezPu239					
TMC	10.00	Sens. Analysis	10.36 pcm	Ratio	0.9937

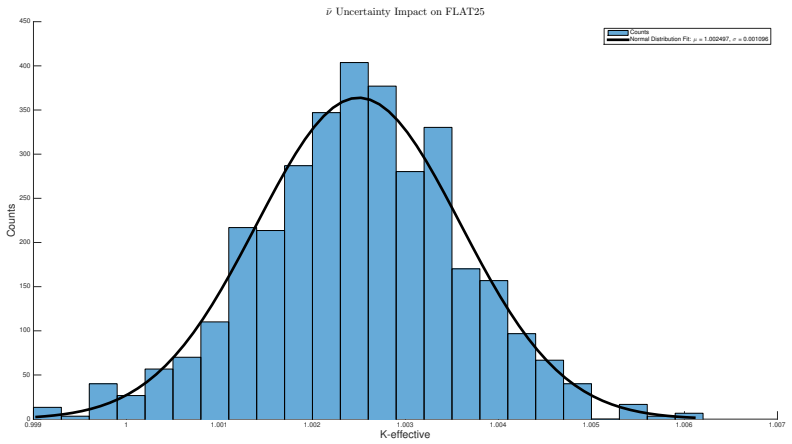

Figure 6.7: $\bar{\nu}$ Uncertainty on FLAT25

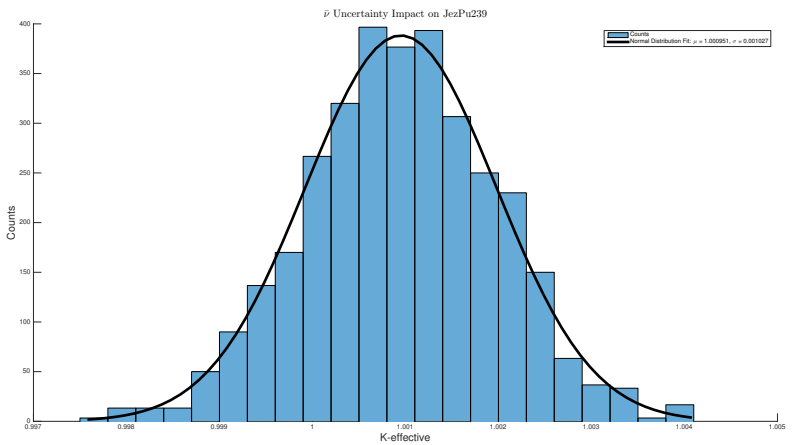

Figure 6.8: $\bar{\nu}$ Uncertainty on JezPu239

6.5 Conclusion

Uncertainties in $\bar{\nu}$ were calculated for various benchmark cases using the Total Monte Carlo method and Sensitivity Analysis. Calculated uncertainties were found to be within 10% of each other. Though there is some uncertainty in $\bar{\nu}$, it is on the order of only 100 pcm; by no means a driving factor in uncertainty of the overall k-effective of a system.

Chapter 7

Fission Neutron Spectra Energy Correlation Impact on k-effective

In a fission reaction, outgoing prompt neutron energies are given by the prompt fission neutron spectrum $\chi(E' \rightarrow E)$. The prompt fission neutron spectrum is a function of the incoming neutron energy and the actinide but has also been found to be a function of the number of neutrons emitted in the fission reaction [19]. In this chapter, the current MCNP6 treatment of prompt fission neutron emission will be discussed along with the implementation of explicit neutron energy correlation in MCNP6 using the LLNL Fission Library. The impacts on k_{eff} for various benchmarks will be discussed.

7.1 Prompt Fission Neutron Energy Treatment in MCNP6

As discussed before, neutron multiplicity for fission is based on the expected value of wgt $\cdot \nu\Sigma_f^{mat}/\Sigma_t^{mat}$ neutrons per collision in the material in criticality calculations. If two or more neutrons are emitted in fission, both their emission energy and direction

are sampled independently; there exists no correlation between the emitted neutron energies or directions.

The prompt fission neutron spectrum used to sample emitted neutron energies is chosen randomly. The probability of choosing a specific isotope's prompt fission energy spectrum is given by

$$P(\chi_{\text{iso}}(E)) = \frac{\nu\Sigma_f^{\text{iso}}}{\nu\Sigma_t^{\text{mat}}}. \tag{7.1}$$

If more than one neutron is emitted in fission, the same spectrum selected before is used to independently sample the energy of the neutrons. MCNP6 does not conserve energy for neutrons emitted in fission.

If explicit neutron multiplicity sampling is enabled, each fission neutron's energy is, by default, sampled independently. There is no explicit energy conservation in this case. However, options in the LLNL Fission Library allow for the implementation of energy correlations, and these options were explored.

7.2 Prompt Fission Neutron Energy Treatment in LLNL Fission Library

The LLNL Fission Library has three different methods for handling fission neutron energy correlations [20]. The default option (`correlation=0`) samples all neutrons emitted in fission independently using the prompt fission spectrum for the isotope that is fissioning. That is, there is no explicit energy conservation in the fission reaction. The second correlation option (`correlation=1`) imposes a total event energy constraint that is a function of the incident neutron energy E_n. The dependence on the incident neutron energy follows from the fact that symmetric binary fission of a nucleus becomes more probable with increasing incident neutron energy. The higher

incident neutron energy can lead to highly excited fission fragments which in turn lead to larger prompt neutron and gamma emissions. The `correlation=1` option calculates the average total fission neutron kinetic energy in the laboratory frame as a function of incident neutron energy [2] based on the Los Alamos Madland-Nix model for three major actinides: uranium-235, uranium-238, and plutonium-239. The average total fission neutron energy for each of the three isotopes are given by the following expressions:

$$\begin{aligned} &< E^{tot}_{neutron} >= 4.838 + 0.3004 E_n \ ^{235}\mathrm{U} \\ &< E^{tot}_{neutron} >= 4.558 + 0.3070 E_n \ ^{238}\mathrm{U} \\ &< E^{tot}_{neutron} >= 6.128 + 0.3428 E_n \ ^{239}\mathrm{Pu} \end{aligned} \tag{7.2}$$

One limitation of the previous method is that it is only applicable to those three major actinides. The `correlation=2` option uses a different method that extends to all major and minor actinides. The method by Vogt [21] fits the quadratic expression of the form

$$< E^{tot}_{n/p} >= c_{n/p} + b_{n/p} E_n + a_{n/p} E_n^2 \tag{7.3}$$

where E_n is the incident neutron energy and the three coefficients are actinide dependent to determine the average total event energy available to neutrons and gamma rays. This correlation option and method were used to study fission neutron energy correlation and their effect on k-effective.

7.3 Fission Neutron Energy Sampling from Correlated Fission Neutron Emission Results

Similar to the MCNP6 Extended Criticality Validation Suite fission multiplicity testing, the suite was subdivided into five cases: plutonium, HEU, IEU, LEU, and uranium-233 cases. Two correlation methods were tested allowing for explicit fission multiplicity sampling: no energy correlation between emitted fission neutrons and imposed total neutron energy conservation from the previously explained correlation option. In addition to k_{eff}, the average neutron energy causing fission was examined to determine the net effect of energy correlation on the fission source.

7.3.1 k_{eff} and Average Energy of Neutron Causing Fission Results for MCNP6 Extended Criticality Validation Suite: Plutonium Systems

Fission neutron energy correlation produces an increase in reactivity for fast plutonium metal systems. A decrease of reactivity for thermal solution systems can be seen in Figure 7.1. The average energy causing fission along with the difference between the two correlation methods can be seen in Figure 7.2. The implementation of neutron fission energy correlation increased the average energy of neutrons causing fission in the system. For fast systems, the increase in the average energy added reactivity to those systems. Thermal systems showed a decrease in reactivity. Differences between energies were found to be on the order of 10 to 60 keV and were especially large for fast systems.

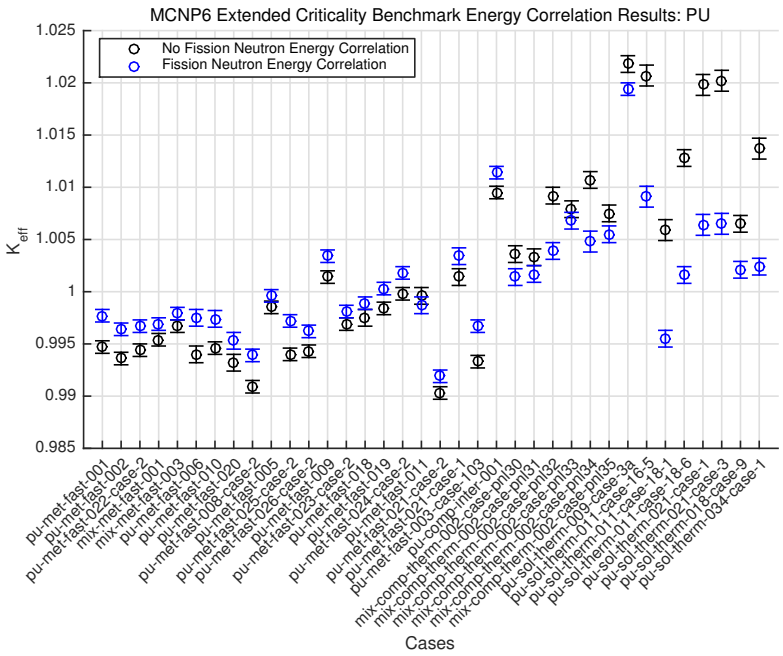

Figure 7.1: k_{eff} Comparisons for Correlated and Uncorrelated Fission Neutron Energy Sampling for Plutonium Systems

7.3.2 k_{eff} and Average Energy of Neutron Causing Fission Results for MCNP6 Extended Criticality Validation Suite: HEU Systems

HEU systems all showed a decrease in reactivity when fission neutron energies were correlated. The differences between the two correlation methods led to negligible differences in the average energy of neutrons causing fission on the order of 10 keV as seen in Figure 7.3.

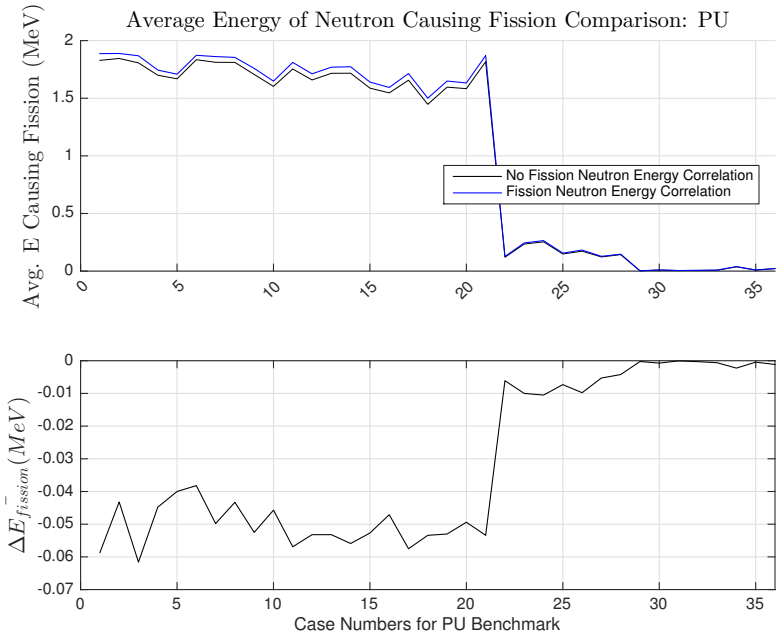

Figure 7.2: Average Energy of Neutron Causing Fission Comparison for Plutonium Systems

7.3.3 k_{eff} and Average Energy of Neutron Causing Fission Results for MCNP6 Extended Criticality Validation Suite: IEU Systems

IEU systems showed a decrease in reactivity with energy correlation for cases as seen in Figure 7.5. The maximal difference in average energy of neutrons causing fission was found to be 25 keV. For both energy correlation options, the differences are negligible though energy correlation reduced the average energy of neutrons causing fission as can be seen in Figure 7.6.

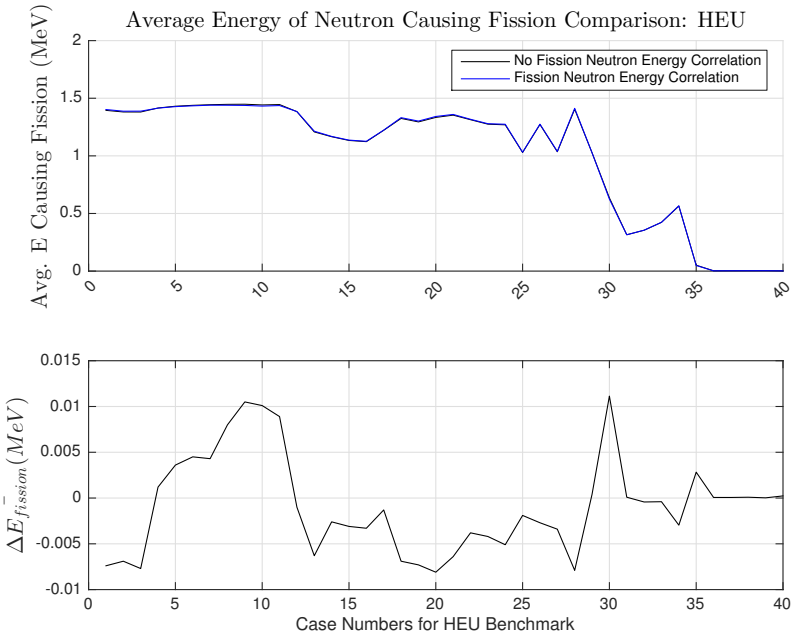

Figure 7.3: Average Energy of Neutron Causing Fission Comparison for HEU Systems

7.3.4 k_{eff} and Average Energy of Neutron Causing Fission Results for MCNP6 Extended Criticality Validation Suite: LEU Systems

LEU systems all showed a decrease in reactivity with fission neutron energy correlation as seen in Table 7.7. All LEU systems are thermal systems and the average energy of neutrons causing fission was found to be almost constant despite correlation of energies indicating thermal systems are less sensitive due to moderation of neutron energies in the systems. Table 7.8 show the differences in the neutron energies to be on the order of 10 keV.

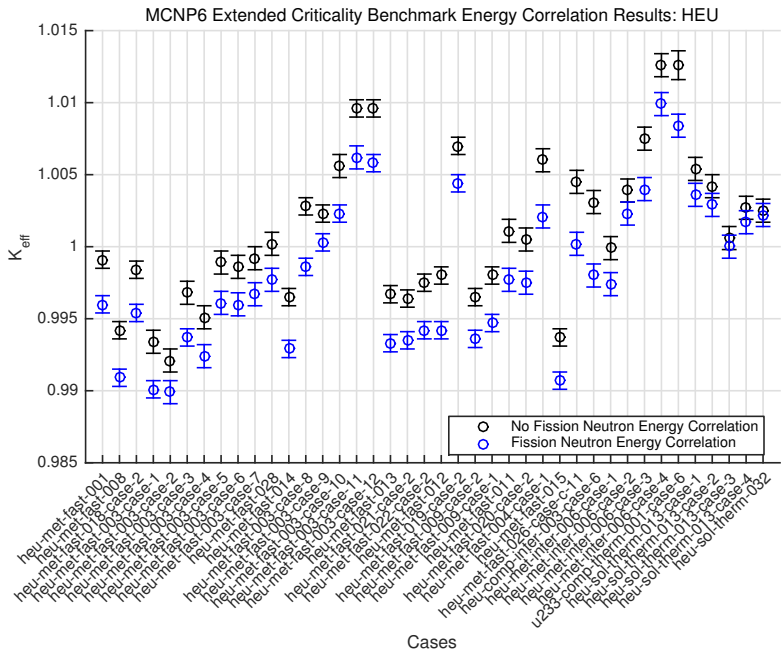

Figure 7.4: k_{eff} Comparisons for Correlated and Uncorrelated Fission Neutron Energy Sampling for HEU Systems

7.3.5 k_{eff} and Average Energy of Neutron Causing Fission Results for MCNP6 Extended Criticality Validation Suite: Uranium-233 Systems

U233 systems all showed a decrease in reactivity. There was an increase in the average energy of neutrons causing fission for fast and intermediate U233 systems as seen in Figure 7.9 with the maximum decrease on the order of 40 keV. Thermal systems show no difference in the average energy of neutrons causing fission as seen in Figure 7.10.

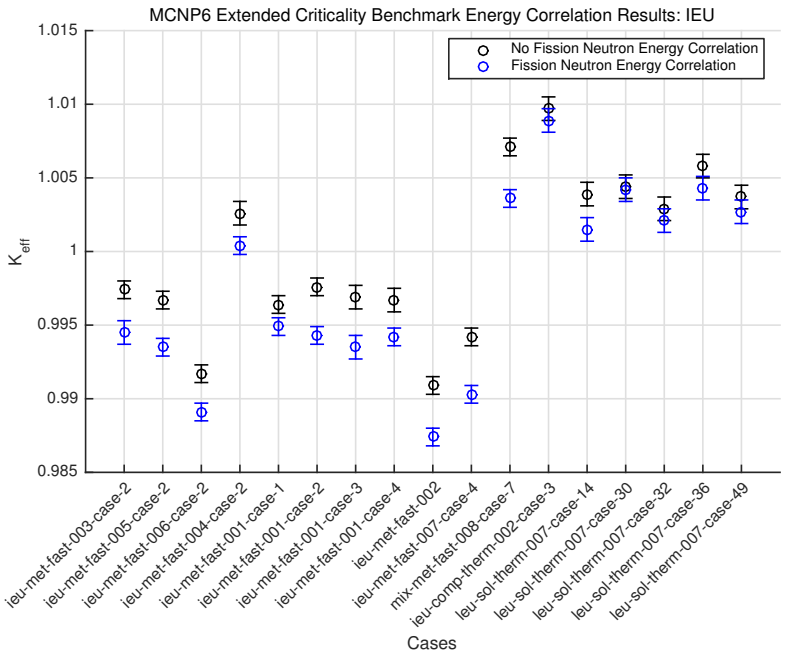

Figure 7.5: k_{eff} Comparisons for Correlated and Uncorrelated Fission Neutron Energy Sampling for IEU Systems

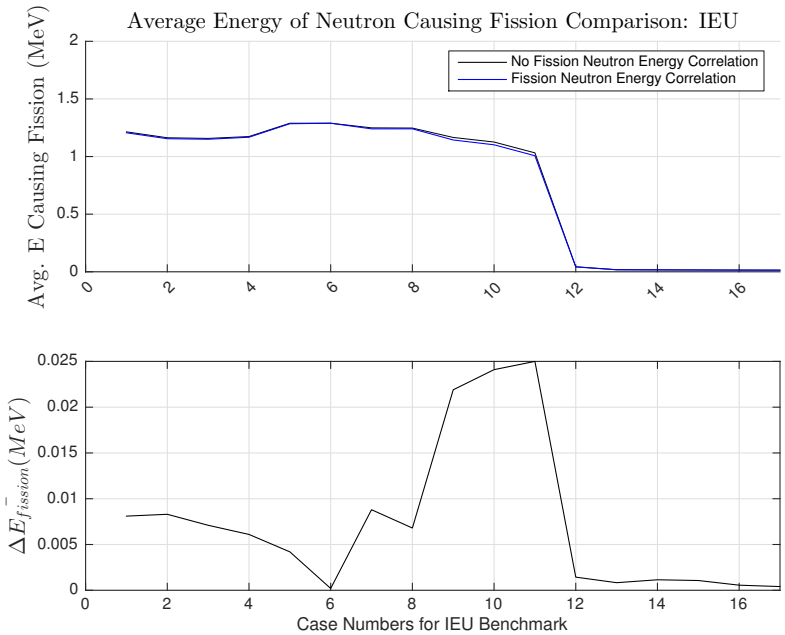

Figure 7.6: Average Energy of Neutron Causing Fission Comparison for IEU Systems

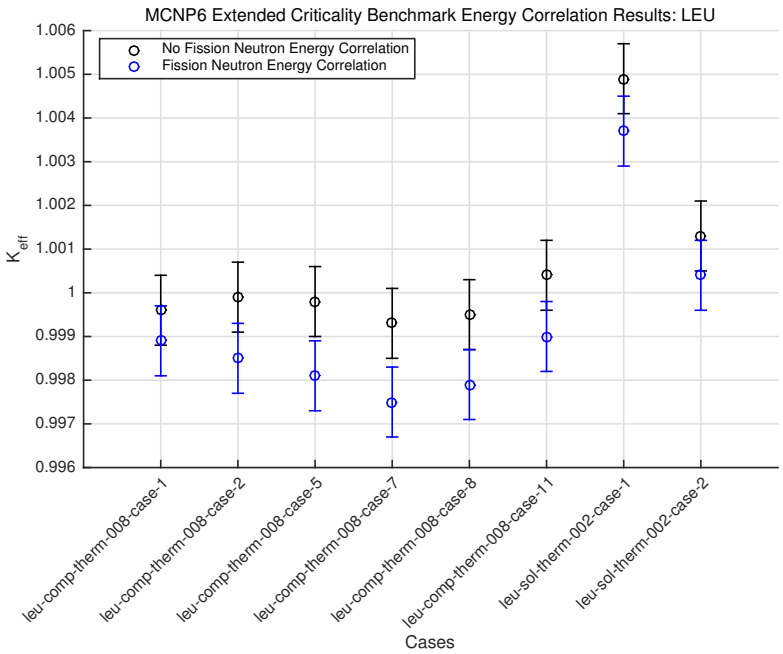

Figure 7.7: k_{eff} Comparisons for Correlated and Uncorrelated Fission Neutron Energy Sampling for LEU Systems

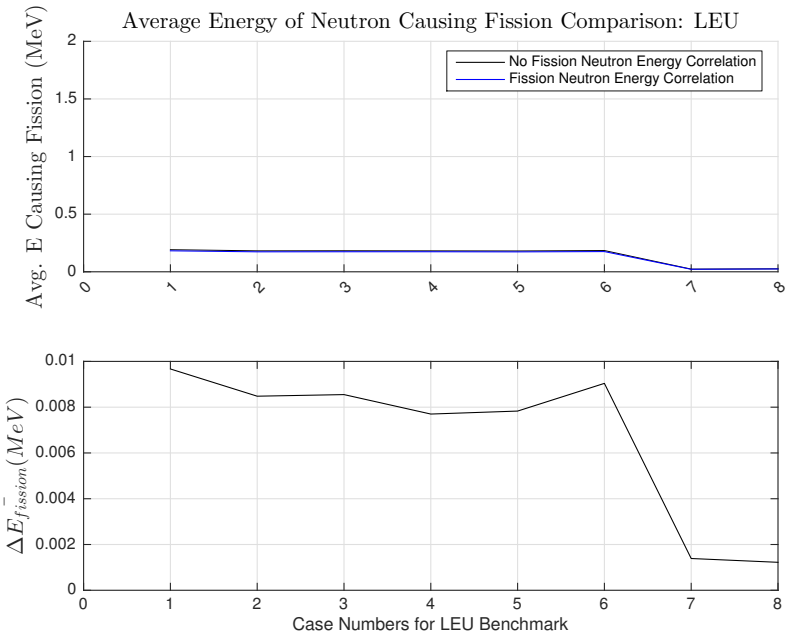

Figure 7.8: Average Energy of Neutron Causing Fission Comparison for LEU Systems

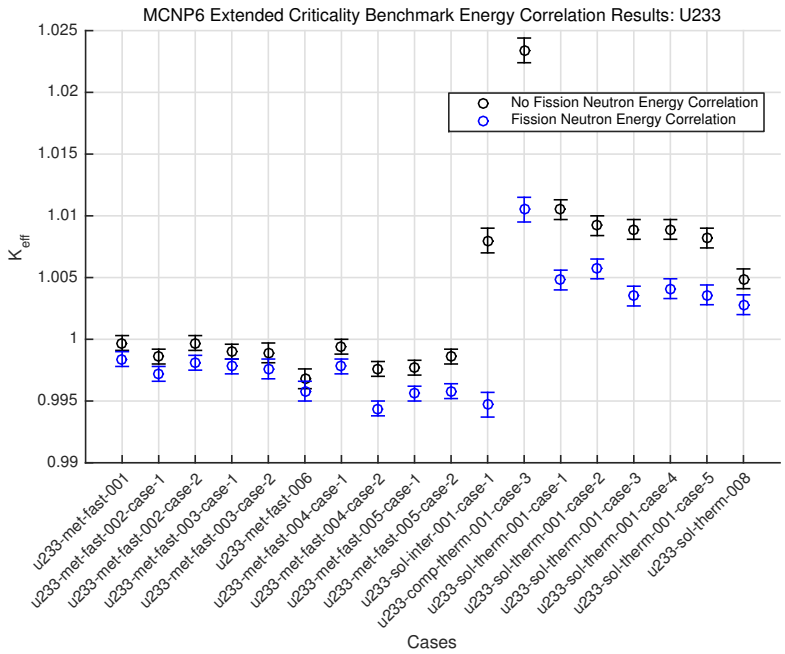

Figure 7.9: k_{eff} Comparisons for Correlated and Uncorrelated Fission Neutron Energy Sampling for U233 Systems

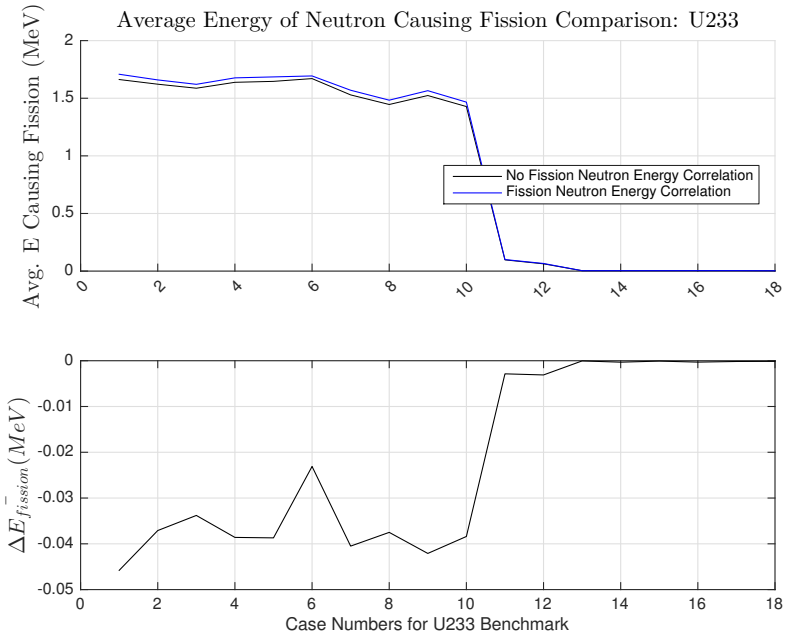

Figure 7.10: Average Energy of Neutron Causing Fission Comparison for U233 Systems

7.4 Conclusion

In the fission process, the energy of neutrons emitted in fission is correlated. The average energy of neutrons born in fission is affected, which then affects absorption reaction rates, fission reaction rates, and the average number of neutrons emitted in fission. These impact the overall k_{eff} of a system. Neutron fission energy correlation was implemented using the method of Terrell [19], and its impact on k_{eff} was investigated for the various systems of the MCNP6 Extended Criticality Benchmark Suite. It was found that fission neutron energy correlation reduced reactivity for all benchmark systems except for fast metal plutonium systems. Fast metal plutonium systems exhibited increased reactivity. Future work should be done to determine the reason for this increase in reactivity. Additional work to determine the effect of energy correlations on k_{eff} needs to be done, and the theoretical impact of energy correlation on k_{eff} determined.

Chapter 8

Conclusions and Future Work

This work focused on the sampling methods used in MCNP6 criticality calculations. With advances in computation methods and resources, the increasing interest in high fidelity modeling of nuclear systems makes it necessary to implement physical models and data that accurately reflect the underlying physics.

For nuclear fission, explicit fission multiplicity data exists for various important actinides. Using the Lawrence Livermore National Laboratory Fission Library, this data was implemented into MCNP6, and MCNP6 was allowed to use explicit fission multiplicity sampling for criticality calculations. Previously no work had been done on explicit fission multiplicity. It was found that explicit multiplicity sampling matched expected-value outcome sampling for most cases with some exceptions. Additional work must be done to determine the cause of the differences for various benchmarks. However, in general, both sampling methods agree with each other.

The propagation of uncertainty in nuclear criticality calculations is of interest, and in this thesis the uncertainty in the average number of neutrons emitted in fission $\bar{\nu}$ was examined. Using the Total Monte Carlo Method and the Sandwich Method using sensitivity coefficients, it was found that sensitivity for $\bar{\nu}$ was small in comparison to other nuclear data parameters. The exercise demonstrated the power of the MCNP6 sensitivity calculation method when combined with covariance data

for actinides.

Lastly, the impact of energy correlation on fission neutron emission energies and its impact on k-effective was examined. It was found that using the correlation method of Terrell [19], that reactivity decreased for all cases except fast metal plutonium systems. Results are highly suggestive of a measurable impact on k-effective due to fission neutron energy correlation. Additional research is necessary to determine the cause of the differences between the correlated and uncorrelated energy implementations. In addition, the use of different energy correlations would be of interest to determine impacts on k-effective.

Appendices

Appendix A

k_{eff} Sensitivity Analysis Input Files

A.1 FLAT23

```
 U233-MET-FAST-006  FLATTOP-23
1         1        0.0475915       -1        $ U-233 Sphere
2         2        0.0480695        1   -2   $ Normal U Reflector
3         0                         2


1         so        4.2058
2         so       24.1194


kcode     5000   1.0     50   250
imp:n     1.0    1.0    0.0
sdef   cel=1  erg=d1
sp1    -3
vol        311.63  58462.76      0.0
area       222.28   7310.43
totnu
#ifdef ENDF7
c ------------------------------------------------- ENDF/B-VII -------
```

```
c         Uranium (98.13 wt.% U-233)
m1         92233     4.6710e-2        92234     5.8772e-4
           92235     1.4158e-5        92238     2.7959e-4
c         Normal Uranium Reflector
m2         92235     3.5050e-4        92238     4.7719e-2
c ------------------------------------------------------------------------
#else
c ------------------------------------------------------ ENDF/B-VI  -------
c         Uranium (98.13 wt.% U-233)
m1         92233.66c     4.6710e-2        92234.66c     5.8772e-4
           92235.66c     1.4158e-5        92238.66c     2.7959e-4
c         Normal Uranium Reflector
m2         92235.66c     3.5050e-4        92238.66c     4.7719e-2
c ------------------------------------------------------------------------
#endif
prdmp    j    999999
print
c
c ***** Nubar Sensitivity *****
c
ksen1 MT=452

 end of input
```

A.2 GODIVA

```
 Godiva  Solid Bare HEU sphere  HEU-MET-FAST-001
1          1        4.7984e-02          -1         imp:n=1
2          0                             1         imp:n=0
```

```
1          so        8.7407

kcode      5000      1.0  50    250
sdef    cel=1      erg=d1     rad=d2     pos=0.0 0.0 0.0
sp1     -3
si2     0.0     8.7407
sp2     -21     2
totnu
#ifdef ENDF7
c ------------------------------------------------------ ENDF/B-VII -------
m1         92234    4.9184e-04      92235    4.4994e-02
           92238    2.4984e-03
c ------------------------------------------------------------------------
#else
c ------------------------------------------------------ ENDF/B-VI  -------
m1         92234.66c    4.9184e-04      92235.66c    4.4994e-02
           92238.66c    2.4984e-03
c ------------------------------------------------------------------------
#endif
prdmp     j     999999
print
c
c ***** Nubar Sensitivity *****
c
ksen1 MT=452

 end of input
```

A.3 ONRL11

```
 ICSBEP U233-SOL-THERM-008  (ORNL-11)
1    1  9.99353e-02    -1
2    2  6.02743e-02    -2   1
3    0                  2

1   so  61.011
2   so  61.786

kcode   5000    1.0    50   250
sdef   cel=1     erg=d1    rad=d2    pos=0.0 0.0 0.0
sp1    -3
si2    0.0   61.011
sp2    -21    2
imp:n   1.0 1.0 0.0
c     uranyl nitrate
#ifdef ENDF7
c ---------------------------------------------------- ENDF/B-VII -------
m1    1001  6.6357e-02
      7014  7.4943e-05
      8016  3.3456e-02      8017  1.3388e-05
     90232  1.4756e-07
     92233  3.3441e-05     92234  5.2503e-07
     92235  1.0184e-08     92238  2.5474e-07
mt1  lwtr.10t
c     al 1100
m2   13027  5.9881e-02
     14028  2.0097e-04     14029  1.0176e-05
     14030  6.7549e-06
```

```
     25055  1.4853e-05     26054  6.4652e-06
     26056  1.0051e-04     26057  2.3012e-06
     26058  3.0682e-07     29063  3.5529e-05
     29065  1.5836e-05
c ------------------------------------------------------------------------
#else
c ------------------------------------------------------ ENDF/B-VI  -------
m1   92233.66c  3.3441e-05     92234.66c  5.2503e-07
     92235.66c  1.0184e-08     92238.66c  2.5474e-07
     90232.66c  1.4756e-07      1001.62c  6.6357e-02
      7014.62c  7.4943e-05      8016.62c  3.3469e-02
mt1  lwtr.60t
c     al 1100
m2   13027.62c  5.9881e-02
     14028.66c  2.0097e-04     14029.62c  1.0176e-05
     14030.66c  6.7549e-06
     25055.62c  1.4853e-05     26054.62c  6.4652e-06
     26056.62c  1.0051e-04     26057.62c  2.3012e-06
     26058.62c  3.0682e-07     29063.62c  3.5529e-05
     29065.62c  1.5836e-05
c ------------------------------------------------------------------------
#endif
prdmp    j     999999
print
c
c ***** Nubar Sensitivity *****
c
ksen1 MT=452

 end of input
```

A.4 PNL33

```
PNL-33: MIX-COMP-THERM-002 sq lattice, pitch=2.20914 cm, 1090.4 PPM
 1   0              21  23 -25 4 -12    fill=11  imp:n=1  $ Cube for Fueled Core
 2   5  1.00160e-1  21 23 -25 (1 -2:14 -15)      imp:n=1  $ Bottom/Top Reflector
 3   6  5.97206e-2  21 23 -25 2 -4               imp:n=1  $ Aluminum Plate
 4   7  3.17234e-2  21 23 -25 12 -14             imp:n=1  $ Lead Shield
 5   0              25:-1:15:-21:-23             imp:n=0  $ Out of core
c     filling universe                           $ Cube cell filled Fuel
 6   0 -32 31 -34 33 lat=1 u=11 imp:n=1 fill=0:32 0:32 0:0
          1 1 1 1 1 1 1 1 1 1 1 1 1 1 1 2 16r
          1 1 1 1 1 1 1 1 1 1 1 1 1 1 1 2 16r
          1 1 1 1 1 1 1 1 1 1 1 1 1 1 1 2 16r
          1 1 1 1 1 1 1 1 1 1 1 1 1 1 1 2 16r
          1 1 1 1 1 1 1 1 1 1 1 1 1 1 2 2 16r
          1 1 1 1 1 1 1 1 1 1 1 1 1 1 2 2 16r
          1 1 1 1 1 1 1 1 1 1 1 1 1 1 2 2 16r
          1 1 1 1 1 1 1 1 1 1 1 1 1 2 2 2 16r
          1 1 1 1 1 1 1 1 1 1 1 1 1 2 2 2 16r
          1 1 1 1 1 1 1 1 1 1 1 1 1 2 2 2 2 16r
          1 1 1 1 1 1 1 1 1 1 1 1 2 2 2 2 2 16r
          1 1 1 1 1 1 1 1 1 1 1 2 2 2 2 2 2 16r
          1 1 1 1 1 1 1 1 1 2 2 2 2 2 2 2 16r
          1 1 1 1 1 1 1 2 2 2 2 2 2 2 2 2 16r
          1 1 1 1 2 2 2 2 2 2 2 2 2 2 2 2 16r
          2 560r
c     fuel cell universe (u=1)
21   1  6.49712e-2   7 -11 -35                u=1 imp:n=1  $ MOX
22   2  6.26175e-2   6 -7  -35                u=1 imp:n=1  $ UO2 layer
```

```
23   3  4.28234e-2   3 -11 -36 #21 #22          u=1 imp:n=1  $ Clad
24   6  5.97206e-2 (5 -8:9 -10) (-37 38:39 -40:41 -42:-43 44)
                                                u=1 imp:n=1  $ Al Egg-Crate
25   5  1.00160e-1   #21 #22 #23 #24 #26        u=1 imp:n=1  $ Moderator
26   3  4.28234e-2   11 -13 -36                 u=1 imp:n=1  $ Plug+Water
c     Part of Radial reflector cell universe (u=2)
31   5  1.00160e-1   #32                        u=2 imp:n=1  $ Water
32   6  5.97206e-2 (5 -8:9 -10) (-37 38:39 -40:41 -42:-43 44)
                                                u=2 imp:n=1  $ Al Egg-Crate


  1   pz -30.0                                    $ bottom of reflector
  2   pz   0.0                                    $ bottom of Al Plate
  3   pz   2.85749                                $ bottom of Fuel Zone
  4   pz   2.8575                                 $ bottom of clad(plug)
  5   pz   3.1750                                 $ bottom of B-eggcrate
  6   pz   3.5560                                 $ bottom of UO2
  7   pz   4.0560                                 $ bottom of PuO2
  8   pz   5.715                                  $ top    of B-eggcrate
  9   pz  92.3925                                 $ bottom of T-eggcrate
 10   pz  94.9325                                 $ top    of T-eggcrate
 11   pz  94.9960                                 $ top    of PuO2 (plug)
 12   pz  95.8215                                 $ top    of clad
 13   pz  95.82151                                $ top    of Fuel Zone
 14   pz  96.774                                  $ top    of lead
 15   pz 110.236                                  $ critical water height
*21   px   0.0                                    $ X-Axis
 22   px  34.241669                               $ X-Fuel Boundary
*23   py   0.0                                    $ Y-Axis
 24   py  34.241669                               $ Y-Fuel Boundary
 25   cz  70.0                                    $ Core Radial Boundary
```

```
 31   px  -1.10457                                  $ - X Cell Boundary
 32   px   1.10457                                  $ + X Cell Boundary
 33   py  -1.10457                                  $ - Y Cell Boundary
 34   py   1.10457                                  $ + Y Cell Boundary
 35   cz   0.64135                                  $ Fuel Outer Radius
 36   cz   0.71755                                  $ Clad Outer Radius
 37   p  1. -1. 0.  1.16204514                      $ - X Cell Boundary
 38   p  1. -1. 0.  1.04709786                      $ - X Cell Boundary
 39   p  1. -1. 0. -1.16204514                      $ - X Cell Boundary
 40   p  1. -1. 0. -1.04709786                      $ - X Cell Boundary
 41   p  1.  1. 0. -1.16204514                      $ - X Cell Boundary
 42   p  1.  1. 0. -1.04709786                      $ - X Cell Boundary
 43   p  1.  1. 0.  1.16204514                      $ - X Cell Boundary
 44   p  1.  1. 0.  1.04709786                      $ - X Cell Boundary

kcode 5000 1.0 50 250
ksrc    0.11     0.11    45.  2.20914  0.11    45.  4.41828  0.11    45.
        6.62742  0.11    45.  8.83656  0.11    45. 11.04570  0.11    45.
       13.25484  0.11    45. 15.46398  0.11    45. 17.67312  0.11    45.
       19.88226  0.11    45. 22.09140  0.11    45. 24.30054  0.11    45.
       26.50968  0.11    45. 28.71882  0.11    45. 30.92796  0.11    45.
       33.13710  0.11    45.
        0.1      2.20914 45.  2.20914  2.20914 45.  4.41828  2.20914 45.
        6.62742  2.20914 45.  8.83656  2.20914 45. 11.04570  2.20914 45.
       13.25484  2.20914 45. 15.46398  2.20914 45. 17.67312  2.20914 45.
       19.88226  2.20914 45. 22.09140  2.20914 45. 24.30054  2.20914 45.
       26.50968  2.20914 45. 28.71882  2.20914 45. 30.92796  2.20914 45.
       33.13710  2.20914 45.
        0.1      4.41828 45.  2.20914  4.41828 45.  4.41828  4.41828 45.
        6.62742  4.41828 45.  8.83656  4.41828 45. 11.04570  4.41828 45.
```

```
13.25484  4.41828 45. 15.46398  4.41828 45. 17.67312  4.41828 45.
19.88226  4.41828 45. 22.09140  4.41828 45. 24.30054  4.41828 45.
26.50968  4.41828 45. 28.71882  4.41828 45. 30.92796  4.41828 45.
33.13710  4.41828 45.
 0.1      6.62742 45.  2.20914  6.62742 45.  4.41828  6.62742 45.
 6.62742  6.62742 45.  8.83656  6.62742 45. 11.04570  6.62742 45.
13.25484  6.62742 45. 15.46398  6.62742 45. 17.67312  6.62742 45.
19.88226  6.62742 45. 22.09140  6.62742 45. 24.30054  6.62742 45.
26.50968  6.62742 45. 28.71882  6.62742 45. 30.92796  6.62742 45.
33.13710  6.62742 45.
 0.1      8.83656 45.  2.20914  8.83656 45.  4.41828  8.83656 45.
 6.62742  8.83656 45.  8.83656  8.83656 45. 11.04570  8.83656 45.
13.25484  8.83656 45. 15.46398  8.83656 45. 17.67312  8.83656 45.
19.88226  8.83656 45. 22.09140  8.83656 45. 24.30054  8.83656 45.
26.50968  8.83656 45. 28.71882  8.83656 45. 30.92796  8.83656 45.
 0.1     11.04570 45.  2.20914 11.04570 45.  4.41828 11.04570 45.
 6.62742 11.04570 45.  8.83656 11.04570 45. 11.04570 11.04570 45.
13.25484 11.04570 45. 15.46398 11.04570 45. 17.67312 11.04570 45.
19.88226 11.04570 45. 22.09140 11.04570 45. 24.30054 11.04570 45.
26.50968 11.04570 45. 28.71882 11.04570 45. 30.92796 11.04570 45.
 0.1     13.25484 45.  2.20914 13.25484 45.  4.41828 13.25484 45.
 6.62742 13.25484 45.  8.83656 13.25484 45. 11.04570 13.25484 45.
13.25484 13.25484 45. 15.46398 13.25484 45. 17.67312 13.25484 45.
19.88226 13.25484 45. 22.09140 13.25484 45. 24.30054 13.25484 45.
26.50968 13.25484 45. 28.71882 13.25484 45. 30.92796 13.25484 45.
 0.1     15.46398 45.  2.20914 15.46398 45.  4.41828 15.46398 45.
 6.62742 15.46398 45.  8.83656 15.46398 45. 11.04570 15.46398 45.
13.25484 15.46398 45. 15.46398 15.46398 45. 17.67312 15.46398 45.
19.88226 15.46398 45. 22.09140 15.46398 45. 24.30054 15.46398 45.
26.50968 15.46398 45. 28.71882 15.46398 45.
```

```
 0.1     17.67312 45.  2.20914 17.67312 45.  4.41828 17.67312 45.
 6.62742 17.67312 45.  8.83656 17.67312 45. 11.04570 17.67312 45.
13.25484 17.67312 45. 15.46398 17.67312 45. 17.67312 17.67312 45.
19.88226 17.67312 45. 22.09140 17.67312 45. 24.30054 17.67312 45.
26.50968 17.67312 45. 28.71882 17.67312 45.
 0.1     19.88226 45.  2.20914 19.88226 45.  4.41828 19.88226 45.
 6.62742 19.88226 45.  8.83656 19.88226 45. 11.04570 19.88226 45.
13.25484 19.88226 45. 15.46398 19.88226 45. 17.67312 19.88226 45.
19.88226 19.88226 45. 22.09140 19.88226 45. 24.30054 19.88226 45.
26.50968 19.88226 45.
 0.1     22.09140 45.  2.20914 22.09140 45.  4.41828 22.09140 45.
 6.62742 22.09140 45.  8.83656 22.09140 45. 11.04570 22.09140 45.
13.25484 22.09140 45. 15.46398 22.09140 45. 17.67312 22.09140 45.
19.88226 22.09140 45. 22.09140 22.09140 45. 24.30054 22.09140 45.
26.50968 22.09140 45.
 0.1     24.30054 45.  2.20914 24.30054 45.  4.41828 24.30054 45.
 6.62742 24.30054 45.  8.83656 24.30054 45. 11.04570 24.30054 45.
13.25484 24.30054 45. 15.46398 24.30054 45. 17.67312 24.30054 45.
19.88226 24.30054 45. 22.09140 24.30054 45. 24.30054 24.30054 45.
 0.1     26.50968 45.  2.20914 26.50968 45.  4.41828 26.50968 45.
 6.62742 26.50968 45.  8.83656 26.50968 45. 11.04570 26.50968 45.
13.25484 26.50968 45. 15.46398 26.50968 45. 17.67312 26.50968 45.
19.88226 26.50968 45. 22.09140 26.50968 45.
 0.1     28.71882 45.  2.20914 28.71882 45.  4.41828 28.71882 45.
 6.62742 28.71882 45.  8.83656 28.71882 45. 11.04570 28.71882 45.
13.25484 28.71882 45. 15.46398 28.71882 45. 17.67312 28.71882 45.
 0.1     30.92796 45.  2.20914 30.92796 45.  4.41828 30.92796 45.
 6.62742 30.92796 45.  8.83656 30.92796 45. 11.04570 30.92796 45.
13.25484 30.92796 45.
 0.1     33.13710 45.  2.20914 33.13710 45.  4.41828 33.13710 45.
```

```
        6.62742 33.13710 45.
mode  n
totnu
#ifdef ENDF7
c ------------------------------------------------- ENDF/B-VII -------
m1     8016 4.3761e-2   8017 1.7512e-5                       $ MOX
      92235 1.4886e-4  92238 2.0611e-2
      92234 1.2458e-6  92236 2.0936e-9  94238 3.8836e-8
      94239 3.9462e-4  94240 3.3206e-5  94241 1.6081e-6
      94242 1.1882e-7  95241 1.4954e-6
m2     8016 4.1926e-2   8017 1.6777e-5                       $ UO2
      92234 1.2406e-6  92235 1.4824e-4  92236 2.0848e-9
      92238 2.0525e-2
m3    24050 3.3101e-6  24052 6.3758e-5  24053 7.2288e-6   $ Clad
      24054 1.7958e-6
      26054 5.5951e-6  26056 8.7752e-5  26057 2.0276e-6
      26058 2.6780e-7
      28058 2.0653e-5  28060 7.9541e-6  28061 3.4583e-7
      28062 1.1012e-6  28064 2.8212e-7
      40090 2.1929e-2  40091 4.7821e-3  40092 7.3095e-3
      40094 7.4075e-3  40096 1.1934e-3
m4     1001 5.6564e-2                                       $ Mod.+Al
       5010 1.0211e-5   5011 4.1356e-5
       8016 2.8349e-2   8017 1.1344e-5
      12024 7.9819e-5  12025 1.0105e-5  12026 1.1126e-5
      13027 8.8588e-3
      14028 4.8390e-5  14029 2.4502e-6  14030 1.6265e-6
      22046 3.1738e-7  22047 2.8622e-7  22048 2.8360e-6
      22049 2.0812e-7  22050 1.9927e-7
      24050 4.1093e-7  24052 7.9153e-6  24053 8.9743e-7
```

```
      24054 2.2294e-7
      25055 3.3528e-6
      26054 9.0043e-7  26056 1.4122e-5  26057 3.2631e-7
      26058 4.3098e-8
      29063 6.6833e-6  29065 2.9788e-6
mt4    lwtr.10t
m5     1001 6.6672e-2                                        $ Mod.
       5010 1.2034e-5   5011 4.8746e-5
       8016 3.3414e-2   8017 1.3371e-5
mt5    lwtr.10t
m6    12024 5.2648e-4  12025 6.6651e-5  12026 7.3383e-5   $ Al
      13027 5.8433e-2
      14028 3.1918e-4  14029 1.6161e-5  14030 1.0728e-5
      22046 2.0934e-6  22047 1.8879e-6  22048 1.8706e-5
      22049 1.3728e-6  22050 1.3144e-6
      24050 2.7105e-6  24052 5.2210e-5  24053 5.9195e-6
      24054 1.4705e-6
      25055 2.2115e-5
      26054 5.9389e-6  26056 9.3145e-5  26057 2.1522e-6
      26058 2.8426e-7
      29063 4.4083e-5  29065 1.9648e-5
m7    82206 7.7539e-3  82207 7.1105e-3  82208 1.6859e-2   $ Lead
m8     1001 5.9914e-2                                        $ Al(Rfl)
       5010 1.0815e-5   5011 4.3805e-5
       8016 3.0028e-2   8017 1.2016e-5
      12024 5.3362e-5  12025 6.7556e-6  12026 7.4379e-6
      13027 5.9226e-3
      14028 3.2352e-5  14029 1.6381e-6  14030 1.0874e-6
      22046 2.1219e-7  22047 1.9136e-7  22048 1.8961e-6
      22049 1.3915e-7  22050 1.3323e-7
```

```
      24050 2.7473e-7  24052 5.2918e-6  24053 5.9998e-7
      24054 1.4905e-7
      25055 2.2415e-6
      26054 6.0197e-7  26056 9.4411e-6  26057 2.1815e-7
      26058 2.8812e-8
      29063 4.4681e-6  29065 1.9915e-6
mt8    lwtr.10t
c ------------------------------------------------------------------------
#else
c ------------------------------------------------------ ENDF/B-VI  -------
m1     8016.62c 4.3779e-2                                                $ MOX
      92235.66c 1.4886e-4  92238.66c 2.0611e-2
      92234.66c 1.2458e-6  92236.66c 2.0936e-9  94238.66c 3.8836e-8
      94239.66c 3.9462e-4  94240.66c 3.3206e-5  94241.66c 1.6081e-6
      94242.66c 1.1882e-7  95241.66c 1.4954e-6
m2     8016.62c 4.1943e-2                                                $ UO2
      92234.66c 1.2406e-6  92235.66c 1.4824e-4  92236.66c 2.0848e-9
      92238.66c 2.0525e-2
m3    24050.62c 3.3101e-6  24052.62c 6.3758e-5  24053.62c 7.2288e-6   $ Clad
      24054.62c 1.7958e-6
      26054.62c 5.5951e-6  26056.62c 8.7752e-5  26057.62c 2.0276e-6
      26058.62c 2.6780e-7
      28058.62c 2.0653e-5  28060.62c 7.9541e-6  28061.62c 3.4583e-7
      28062.62c 1.1012e-6  28064.62c 2.8212e-7
      40000.66c 4.2621e-2
m4     1001.62c 5.6564e-2                                                $ Mod.+Al
       5010.66c 1.0211e-5   5011.66c 4.1356e-5
       8016.62c 2.8360e-2
      12000.62c 1.0105e-4
      13027.62c 8.8588e-3
```

```
      14028.66c 4.8390e-5  14029.62c 2.4502e-6  14030.66c 1.6265e-6
      22000.62c 3.8470e-6
      24050.62c 4.1093e-7  24052.62c 7.9153e-6  24053.62c 8.9743e-7
      24054.62c 2.2294e-7
      25055.62c 3.3528e-6
      26054.62c 9.0043e-7  26056.62c 1.4122e-5  26057.62c 3.2631e-7
      26058.62c 4.3098e-8
      29063.62c 6.6833e-6  29065.62c 2.9788e-6
mt4   lwtr.60t
m5     1001.62c 6.6672e-2                                        $ Mod.
       5010.66c 1.2034e-5   5011.66c 4.8746e-5
       8016.62c 3.3427e-2
mt5   lwtr.60t
m6    12000.62c 6.6651e-4                                        $ Al
      13027.62c 5.8433e-2
      14028.66c 3.1918e-4  14029.62c 1.6161e-5  14030.66c 1.0728e-5
      22000.62c 2.5375e-5
      24050.62c 2.7105e-6  24052.62c 5.2210e-5  24053.62c 5.9195e-6
      24054.62c 1.4705e-6
      25055.62c 2.2115e-5
      26054.62c 5.9389e-6  26056.62c 9.3145e-5  26057.62c 2.1522e-6
      26058.62c 2.8426e-7
      29063.62c 4.4083e-5  29065.62c 1.9648e-5
m7    82206.66c 7.7539e-3  82207.66c 7.1105e-3  82208.66c 1.6859e-2   $ Lead
m8     1001.62c 5.9914e-2                                        $ Al(Rfl)
       5010.66c 1.0815e-5   5011.66c 4.3805e-5
       8016.62c 3.0040e-2
      12000.62c 6.7556e-5
      13027.62c 5.9226e-3
      14028.66c 3.2352e-5  14029.62c 1.6381e-6  14030.66c 1.0874e-6
```

```
      22000.62c 2.5720e-6
      24050.62c 2.7473e-7  24052.62c 5.2918e-6  24053.62c 5.9998e-7
      24054.62c 1.4905e-7
      25055.62c 2.2415e-6
      26054.62c 6.0197e-7  26056.62c 9.4411e-6  26057.62c 2.1815e-7
      26058.62c 2.8812e-8
      29063.62c 4.4681e-6  29065.62c 1.9915e-6
mt8   lwtr.60t
c ------------------------------------------------------------------------
#endif
prdmp j   999999
print
c
c ***** Nubar Sensitivity *****
c
ksen1 MT=452

 end of input
```

A.5 JEZPU

```
 Jezebel  PU-MET-FAST-001  solid bare Pu sphere
1         1        0.040290        -1        $ Pu Sphere
2         0                         1


1         so       6.3849


kcode     5000   1.0  50   250
imp:n     1.0    0.0
sdef   cel=1  erg=d1
```

```
sp1    -3
vol       1090.31      0.0
area       512.29
totnu
#ifdef ENDF7
c ------------------------------------------------- ENDF/B-VII -------
m1        31069     8.2663e-4          31071     5.4857e-4
          94239     3.7047e-2          94240     1.7512e-3
          94241     1.1674e-4
c ------------------------------------------------------------------------
#else
c ------------------------------------------------- ENDF/B-VI  -------
m1        31000.66c     1.3752e-3
          94239.66c     3.7047e-2
          94240.66c     1.7512e-3
          94241.66c     1.1674e-4
c ------------------------------------------------------------------------
#endif
prdmp    j    999999
print
c
c ***** Nubar Sensitivity *****
c
ksen1 MT=452

 end of input
```

Appendix B

ACE Data File Writer MATLAB Script for Uncertainty Analysis

B.1 Uranium-235 Correlated $\bar{\nu}$ ACE File Writer

```
%ACE Data File Creator-U235
%Covariance Data: U-235 (ENDF/B-VII.1)

clc, clear, clf, close all

addpath('/Volumes/MarioPassportMac/JezPu239MCNP');
addpath(['/Users/mario/Documents/MCNP_UncertQuant/'...
    'ActinideCovarianceNu']);

%Read Original ACE Data File and Covariance Data
ACE = textread('92235.710nc','%s','delimiter','\n',...
    'whitespace', '');
```

```
13 U235Data = ...
       textread('92235NuBarCovMod','%f','delimiter','\n'...
14      ,'whitespace', '');
15
16 Eact = load('U235Energy');
17 nutotact = load('U235nutot');
18 Ecov = load('92235.nucov')./1e6;
19
20 for i = 1:length(Ecov)-1
21
22      Ebin(i,1) = Ecov(i);
23      Ebin(i,2) = Ecov(i+1);
24
25 end
26
27 Eint = mean(Ebin,2);
28
29 %nutot interpolation function
30 nuintep = @(x) interp1(Eact,nutotact,x);
31 nuint = nuintep(Eint);
32
33 NEU235 = 16;
34
35 k = 0;
36
37 U235CovMatrix = zeros(NEU235-1,NEU235-1);
38
39 for i = 1:NEU235-1
40
41      for j = (1+(i-1)):NEU235-1
```

```
42
43          k = k + 1;
44
45          U235CovMatrix(i,j) = U235Data(k);
46
47      end
48
49  end
50
51  U235CovMatrix = U235CovMatrix + triu(U235CovMatrix,1)';
52  C = U235CovMatrix;
53
54  [vec,val] = eig(U235CovMatrix);
55  val(val<0) = eps;
56  U235CovMatrix = vec*val*vec';
57
58  CholU235 = chol(U235CovMatrix);
59
60  nutotline0 = 95724;
61  nutotline1 = 95744;
62
63  for k = 1:1000
64
65      if i > 1
66
67          clear nurand
68
69      end
70
71  R = randn(1,length(CholU235));
```

```
72
73 nurand = R*CholU235 + nuint';
74
75 %Extrapolation and Interpolation of Nu Values over entire ...
      energy range
76 nunew = interp1(Eint,nurand,Eact,'linear','extrap');
77
78 nunew(3:end+2) = nunew;
79 nunew(1) = 1.95e1;
80 nunew(2) = 2.00e1;
81 nunew(end+1) = 16;
82 nunew(end+1) = 17;
83 nunew(end+1) = 18;
84
85 nunew = reshape(nunew,[4 length(nunew)/4])';
86
87 dim = size(nunew);
88
89 for i = 1:dim(1)
90
91     if i ~= dim(1)
92
93         s{i}=sprintf('   %3.11E   %3.11E   %3.11E   ...
              %3.11E', nunew(i,:));
94
95     else
96
97         s{i}=sprintf('   %3.11E                  %i ...
                          %i                  %i', ...
              nunew(i,:));
```

```
98
99      end
100
101 end
102
103 for i = nutotline0:nutotline1
104
105     ACE{i} = s{i-(nutotline0-1)};
106
107 end
108
109 %Location of ACE file to be modified
110 file = dir;
111
112 fid = fopen(file,'w');
113
114 for i = 1:length(ACE)
115
116     fprintf(fid,ACE{i});
117     fprintf(fid,'\n');
118
119 end
120
121 fprintf('Data File %i Created \n',k);
122 fclose(fid);
123
124 end
```

B.2 Uranium-238 Correlated $\bar{\nu}$ ACE File Writer

```
%ACE Data File Creator-U238
%Covariance Data: U-238 (ENDF/B-VII.1)

clc, clear, clf, close all

ACE = textread('92238.710nc','%s','delimiter',...
    '\n','whitespace', '');
nulinestart = 197205;
nulinefin = 197207;

NE = 6;

Ein = [1.00000000000E-11 2.53000000000E-08...
    2.90000000000E+00   4.00000000000E+00...
    5.15000000000E+00 6.00000000000E+00...
    8.00000000000E+00   9.00000000000E+00...
    1.58500000000E+01 3.00000000000E+01];
nuin = [2.49208800000E+00   2.49208800000E+00...
    2.69876900000E+00 2.90860400000E+00...
    3.12383700000E+00   3.24999100000E+00...
    3.54028900000E+00 3.68842300000E+00...
    4.72780100000E+00   6.41410900000E+00];

y = @(x) interp1(Ein,nuin,x,'linear','extrap');

E = {'1.000000E-5';'1.000000E+6';'4.000000E+6';...
```

```
27      '1.000000E+7';'2.000000E+7';'3.000000E+7'};
28  En = cellfun(@str2num,E)./1e6;
29
30  for i = 1:length(En)-1;
31
32      Ebin(i,1) = En(i);
33      Ebin(i,2) = En(i+1);
34
35  end
36
37  Ebin(end,2) = En(end);
38
39  Eint = mean(Ebin,2);
40
41  nuint = y(Eint);
42
43  FracCov = [0.00040000000000000;
44             0;
45             0;
46             0;
47             0;
48             0.00017857590000000;
49             7.99440600000000e-05;
50             5.57172400000000e-05;
51             0;
52             0.00020762650000000;
53             9.64307400000000e-05;
54             0;
55             0.00020077720000000;
56             0;
```

```
57              0.0006534219000000000];
58
59  U238CovMatrix = zeros(NE-1,NE-1);
60
61  k = 0;
62
63  for i = 1:NE-1
64
65      for j = (1+(i-1)):NE-1
66
67          k = k + 1;
68
69          U238CovMatrix(i,j) = FracCov(k)*nuint(i)*nuint(j);
70
71      end
72
73  end
74
75  U238CovMatrix = U238CovMatrix + triu(U238CovMatrix,1)';
76
77  CholU238 = chol(U238CovMatrix);
78
79  for k = 1:1000
80
81      if i > 1
82
83          clear nurand
84
85      end
86
```

```
87  R = randn(1,length(CholU238));
88
89  nurand = R*CholU238 + nuint';
90
91  %Extrapolation and Interpolation of Nu Values over entire ...
       energy range
92  nunew = interp1(Eint,nurand,Ein,'linear','extrap');
93  nunew(2:end+1)= nunew(1:end);
94  nunew(1) = 30;
95  nunew(end+1) = 16;
96
97  nunew = reshape(nunew,[4 length(nunew)/4])';
98
99  dim = size(nunew);
100
101 for i = 1:dim(1)
102
103     if i == dim(1)
104
105         s{i}=sprintf('   %3.11E   %3.11E   %3.11E ...
                              %i', nunew(i,:));
106
107     else
108
109         s{i}=sprintf('   %3.11E   %3.11E   %3.11E   ...
               %3.11E', nunew(i,:));
110
111     end
112
113 end
```

```
114
115 for i = nulinestart:nulinefin
116
117     ACE{i} = s{i-(nulinestart-1)};
118
119 end
120
121 %Location of ACE file to be modified
122 file = dir;
123
124 %fid = fopen(file,'w');
125 fid = fopen(file,'w');
126
127 for i = 1:length(ACE)
128
129     fprintf(fid,ACE{i});
130     fprintf(fid,'\n');
131
132 end
133
134 fprintf('Data File %i Created \n',k);
135 fclose(fid);
136
137 end
```

B.3 Plutonium-239 Correlated $\bar{\nu}$ ACE File Writer

```
1 %ACE Data File Creator-Pu239
```

```
%Covariance Data: Pu-239 (ENDF/B-VII.1)

clc, clear

ACE = textread('94239.710nc','%s','delimiter',...
    '\n','whitespace', '');
nulinestart = 92126;
nulinefin = 92807;

data_vec = load('Pu239cov.txt');

Etot = load('Etot.nu');
a = size(Etot);

nutot = load('nutot.nu');
b = size(nutot);

Etot = reshape(Etot',a(1)*a(2),1);
Etot(1) = []; Etot(1)=[];

nutot = reshape(nutot',b(1)*b(2),1);
nutot(end) = []; nutot(end) = [];

Ecov = load('Ecov.txt')./1e6;

for i = 1:length(Ecov)-1

    CovarEne(i,1) = Ecov(i);
    CovarEne(i,2) = Ecov(i+1);

```

```
32 end
33
34 Einterp = mean(CovarEne,2);
35
36 nuinterp = interp1(Etot,nutot,Einterp);
37
38 dims = size(data_vec);
39
40 covele = reshape(data_vec',dims(1)*dims(2),1);
41 covele(1:3) = [];
42
43 %From ENDF/B-VII.1 File for Pu-239
44 %See ENDF manual: ...
      http://www.nndc.bnl.gov/csewg/docs/endf-manual.pdf
45 %Page: 264
46
47 NE = 51;
48
49 covmat = zeros(NE-1,NE-1);
50
51 k = 0;
52
53 %Upper Triangular Matrix
54
55 for i = 1:NE-1
56
57     for j = i:NE-1
58
59         k = k + 1;
60         covmat(i,j) = covele(k)*nuinterp(i)*nuinterp(j);
```

```
61
62      end
63
64  end
65
66  %Creates symmetric covariance matrix
67  Sigma = covmat + triu(covmat,1)';
68
69  % Note: Sigma only positive definite for ...
        Sigma(2:end,2:end). First
70  % location in matrix presents a problem. Ignoring first ...
        data point for now.
71
72  Sigma = Sigma(2:end,2:end);
73
74  lambda = sort(eig(Sigma),'descend')./max(eig(Sigma));
75
76  CholCov = chol(Sigma);
77
78  %Erasing first data point of interpolate nu values
79  nuinterp(1) = [];
80  Einterp(1) = [];
81
82  for k = 1:1000
83
84      if i > 1
85
86          clear nurand
87
88      end
```

```
89
90 nurand = randn(1,length(CholCov));
91
92 %Extrapolation and Interpolation of Nu Values over entire ...
      energy range
93 nunew = interp1(Einterp,nurand,Etot,'linear','extrap');
94 nunew(end+1) = 16;
95 nunew(end+1) = 17;
96
97 nunew = reshape(nunew,[4 length(nunew)/4])';
98
99 for i = 1:length(nunew)
100
101     if i == length(nunew)
102
103         s{i}=sprintf('   %3.11E   %3.11E                    ...
              %i                   %i', nunew(i,:));
104
105     else
106
107         s{i}=sprintf('   %3.11E   %3.11E   %3.11E   ...
              %3.11E', nunew(i,:));
108
109     end
110
111 end
112
113 for i = nulinestart:nulinefin
114
115     ACE{i} = s{i-(nulinestart-1)};
```

```
116
117 end
118
119 %Location of ACE file to be modified
120 file = dir;
121
122 fid = fopen(file,'w');
123
124 for i = 1:length(ACE)
125
126     fprintf(fid,ACE{i});
127     fprintf(fid,'\n');
128
129 end
130
131 fprintf('Data File %i Created \n',k);
132 fclose(fid);
133
134 end
```

Bibliography

[1] Alhassan, E., Sjöstrand, H., Duan, J., Gustavsson, C., Koning, A., Pomp, S., Rochman, D., and Österlund, M. "Combining Total Monte Carlo and Benchmarks for Nuclear Data Uncertainty Propagation on an LFR's Safety Parameters". In: *Proceedings of ND2013, Nucl. Data Sheets (accepted) (2014)* (2013).

[2] Beck, B., Brown, D. A., Daffin, F., Hedstrom, J., and Vogt, R. *Implementation of Energy-Dependent Q Values for Fission*. Tech. rep. UCRL-TR-234617, Lawrence Livermore National Laboratory, 2007.

[3] Briggs, J. B., Dean, V. F., and Scott, L. "The International Criticality Safety Benchmark Evaluation Project (ICSBEP)". In: *Experimental Needs In Criticality Safety* (2003), p. 109.

[4] Broadhead, B. L., Rearden, B. T., Hopper, C. M., Wagschal, J. J, and Parks, C. V. "Sensitivity and Uncertainty-Based Criticality Safety Validation Techniques". In: *Nuclear Science and Engineering* 146.3 (2004), pp. 340–366.

[5] Brown, F. B. and Sutton, T. M. *Monte Carlo Fundamentals*. Tech. rep. Knolls Atomic Power Laboratory, Schenectady, NY (United States), 1996.

[6] Cullen, D. E. *Sampling the Number of Neutrons Emitted per Fission*. Tech. rep. UCRL-TR-222526, Lawrence Livermore National Laboratory, Livermore, CA (United States), 2006.

[7] Duderstadt, J. J. and Hamilton, L. J. *Nuclear Reactor Analysis*. John Wiley and Sons, Inc., New York, 1976.

[8] Dupree, S. A. and Fraley, S. K. *A Monte Carlo primer: A Practical Approach to Radiation Transport*. Springer Science & Business Media, 2012.

[9] Gwin, R., Spencer, R. R., and Ingle, R. W. "Measurements of the Energy Dependence of Prompt Neutron Emission from U-233, U-235, Pu-239, and Pu-241 for $E_n = 0.005$ to 10 eV Relative to Emission from Spontaneous Fission of Cf-252". In: *Nuclear Science and Engineering* 87.4 (1984), pp. 381–404.

[10] Herman, M. "ENDF-6 Formats Manual. Data Formats and Procedures for the Evaluated Nuclear Data File ENDF/B-VI and ENDF/B-VII". In: (2009).

[11] Holden, N. E. and Zucker, M. S. *Reevaluation of the Average Prompt Neutron Emission Multiplicity ($\bar{\nu}$) Values from Fission of Uranium and Transuranium Nuclides*. Tech. rep. Brookhaven National Laboratory, Upton, NY (United States), 1984.

[12] Howerton, R. J. *The LLL Evaluated Nuclear Data Library (ENDL): Evaluation Techniques, Reaction Index, and Descriptions of Individual Evaluations*. Lawrence Livermore National Laboratory, 1975.

[13] Kiedrowski, B. C. *MCNP6.1 k-Eigenvalue Sensitivity Capability: A Users' Guide*. Tech. rep. LA-UR-13-22251. Los Alamos National Laboratory, Los Alamos, NM (United States), 2013.

[14] Lewis, E. E. and Miller, W. F. *Computational Methods of Neutron Transport*. 1984.

[15] Lieberoth, J. *Monte Carlo Technique to Solve the Static Eigenvalue Problem of the Boltzmann Transport Equation.* Tech. rep. Interatom, Bensberg, Ger., 1968.

[16] Mendelson, M.R. "Monte Carlo Criticality Calculations for Thermal Reactors". In: *Nuclear Science and Engineering* 32.3 (1968), pp. 319–331.

[17] Rising, M. E., Prinja, A. K., and Talou, P. "Prompt Fission Neutron Spectrum Uncertainty Propagation Using Polynomial Chaos Expansion". In: *Nuclear Science and Engineering* 175.2 (2013), pp. 188–203.

[18] Rochman, D., Koning, A. J., van der Marck, S. C., Hogenbirk, A., and van Deen, D. "Nuclear Data Uncertainty Propagation: Total Monte Carlo vs. Covariances". In: *Journal of Korean Physical Society (Proceedings of International Conference on Nuclear Data for Science and Technology, ND2010)*. Vol. 59. 2. 2011, pp. 1236–1241.

[19] Terrell, J. "Distributions of Fission Neutron Numbers". In: *Physical Review* 108.3 (1957), p. 783.

[20] Verbeke, J. M., Hagmann, C., and Wright, D. *Simulation of Neutron and Gamma Ray Emission from Fission and Photofission*. Tech. rep. UCRL-AR-228518. Lawrence Livermore National Laboratory, Livermore, CA (United States), 2010.

[21] Vogt, R. *Energy-Dependent Fission Q Values Generalized for All Actinides*. Tech. rep. LLNL-TR-407620, Lawrence Livermore National Laboratory, Livermore, CA (United States), 2008.

[22] Zucker, M. S. and Holden, N. E. "Energy Dependence of Neutron Multiplicity P_ν in Fast-Neutron-Induced Fission for U-235, U-238, and Pu-239". In: BNL-38491 (1986).